



**VICTORIA UNIVERSITY**  
MELBOURNE AUSTRALIA

*Optimization of solar farm design for energy efficiency in university campuses using machine learning: A case study*

This is the Published version of the following publication

Assareh, Ehsanolah, Izadyar, Nima, Jamei, Elmira, Monzavian, Mohammad amin, Agarwal, Saurabh and Pak, Wooguil (2025) Optimization of solar farm design for energy efficiency in university campuses using machine learning: A case study. *Engineering Applications of Artificial Intelligence*, 153. ISSN 0952-1976

The publisher's official version can be found at  
<https://www.sciencedirect.com/science/article/pii/S0952197625008474?via%3Dihub>  
Note that access to this version may require subscription.

Downloaded from VU Research Repository <https://vuir.vu.edu.au/49388/>



# Optimization of solar farm design for energy efficiency in university campuses using machine learning: A case study

Ehsanolah Assareh<sup>a,b,1</sup>, Nima Izadyar<sup>b,c,1,\*</sup>, Elmira Jamei<sup>b,c</sup>, Mohammad amin Monzavian<sup>a</sup>, Saurabh Agarwal<sup>d,1</sup>, Wooguil Pak<sup>d,\*\*</sup>

<sup>a</sup> Department of Renewable Energy Technology, Materials and Energy Research Center, Dez.C., Islamic Azad University, Dezful, Iran

<sup>b</sup> Built Environment and Engineering Program, College of Sport, Health and Engineering (CoSHE), Victoria University, Melbourne, Australia

<sup>c</sup> Institute for Sustainable Industries and Liveable Cities, Victoria University, Melbourne, VIC, 3011, Australia

<sup>d</sup> Department of Information and Communication Engineering, Yeungnam University, Gyeongsan, 38541, South Korea

## ARTICLE INFO

### Keywords:

Educational facility energy efficiency  
Machine learning applications in energy optimization  
Multi-objective optimization  
Response surface methodology  
Solar-powered multi-generation systems  
Net-zero energy systems

## ABSTRACT

The increasing energy demand in multifunctional buildings, like university buildings, hinders sustainability and cost efficiency. This study addresses this issue by designing and optimizing a multi-generation solar farm using Machine Learning to enhance system performance and reduce costs. By framing Response Surface Methodology (RSM) as an interpretable supervised machine learning technique, this study combines it with the Building Energy Optimization Tool (BEopt) and Engineering Equation Solver (EES) for data modeling and optimization. The integration leverages RSM's computational efficiency to optimize exergy efficiency and cost. The novelty lies in enhancing renewable energy integration in large-scale educational facilities, an underexplored domain, using Machine Learning-driven Multi-Objective Optimization. A university building in a cooling-dominant extreme climate was selected, with annual energy demands of 18.24 Gigawatt hours (GWh) for electricity, 6.57 GWh for heating, and 7.52 GWh for cooling. A multi-generation solar farm is proposed and optimized to meet this demand and provide surplus energy, which can be stored, utilized for additional applications, or exported to the grid. The optimized solar farm generates 22.8 GWh of electricity, 17.9 GWh of heating, and 12.9 GWh of cooling, achieving an exergy efficiency of 25.69 % with an operational cost of \$10.15 per hour, and a CO<sub>2</sub> emissions reduction of 7395 metric tons per year. This study provides a scalable and modular framework for optimizing energy management in high-demand environments, contributing to sustainability goals and energy-efficient buildings. Future studies may explore dynamic climate variations, real-time demand forecasting, and hybrid renewable energy sources to improve system resilience, adaptability, and sustainability.

## 1. Introduction

The environmental impact of fossil fuel-based energy use in buildings, which contributes to global warming, air pollution, and resource depletion, has driven the urgent need for sustainable energy solutions, particularly the adoption of renewable energy sources (Arshad et al., 2024; IEA, 2024; UNEP, 2023). Buildings are responsible for approximately 37 % of global energy consumption, making Zero-Energy Buildings (ZEBs) a critical strategy for considerably reducing emissions and energy dependency through the integration of renewable

energy technologies (Jaysawal et al., 2022; Lou and Hsieh, 2024; Li et al., 2013). Several studies have demonstrated the successful implementation of ZEBs in minimizing environmental impact, specifically highlighting their role in reducing CO<sub>2</sub> emissions (Sadat et al., 2024; Maleki Dastjerdi et al., 2024). Multi-generation systems, in particular, play a crucial role in achieving ZEB targets by simultaneously providing electricity, heating, and cooling, thereby enhancing energy resilience, improving cost-effectiveness, and reducing environmental impacts (Temiz and Dincer, 2022; Aljashaami et al., 2024; Mohammadiakhah et al., 2021). Research findings indicate that multi-generation systems

\* Corresponding author. Built Environment and Engineering Program, College of Sport, Health and Engineering (CoSHE), Victoria University, Melbourne, Australia.

\*\* Corresponding author.

E-mail addresses: [nima.izadyar@vu.edu.au](mailto:nima.izadyar@vu.edu.au) (N. Izadyar), [wooguilpak@yu.ac.kr](mailto:wooguilpak@yu.ac.kr) (W. Pak).

<sup>1</sup> These authors contributed equally to this article as the first author.

further strengthen resilience by increasing both energy and exergy efficiency while significantly lowering CO<sub>2</sub> emissions (Assareh et al., 2025a).

Solar energy remains a key component of ZEB design due to its scalability, wide availability, and ability to generate on-site clean energy, reducing reliance on conventional grids (Ye et al., 2023; Sarvar-Ardeh et al., 2024; Shayan, 2020). Solar-driven multi-generation systems offer additional advantages due to their ability to supply clean energy on-site while maintaining scalability (Noro et al., 2021; Sami et al., 2024; Wang et al., 2024a; Almatrafi and Khaliq, 2021). Previous studies demonstrate that integrating photovoltaic (PV) panels with other energy sources, such as wind power (Lykas et al., 2023; Baniasadi et al., 2023; Kyriaki and Giama, 2022) and advanced storage technologies (Assareh et al., 2025b; Lamnatou et al., 2022), improves system stability and ensures a continuous energy supply, even during periods of low solar output (Mohammadi et al., 2020; Chandel et al., 2022). Furthermore, renewable energy multi-generation systems, including solar-driven configurations, have proven effective in supplying energy for high-demand built environments, particularly in large-scale applications in extreme climates where substantial cooling and heating loads can lead to partial or total blackouts due to energy supply disruptions (Gonçalves et al., 2024; Nedaei et al., 2022). However, designing these systems for large-scale multifunctional applications, such as university campuses in extreme climates, remains underexplored, likely due to challenges such as optimizing system configurations, ensuring economic feasibility, and improving long-term operational performance (Xu et al., 2024; Munguba et al., 2024). Addressing these challenges requires advanced modeling and optimization techniques capable of systematically balancing competing objectives, including energy efficiency, cost, and system resilience.

Multi-Objective Optimization (MOO) approaches have emerged as effective tools for improving the design and performance of solar-driven multi-generation systems, enabling more efficient integration of renewable energy sources while optimizing key cost, performance, and environmental metrics, such as energy cost, energy and exergy efficiency, and CO<sub>2</sub> emission reduction (Auza et al., 2024; Chen, 2023; Nam et al., 2025). The literature shows that MOO approaches encompass machine learning algorithms and artificial intelligence-based techniques, such as Genetic Algorithms (GAs) and Artificial Neural Networks (ANNs) (Wang et al., 2024b; Zhang et al., 2024a; Dashtizadeh and Houshfar, 2025), as well as mathematical methods like Kalman filtering (Wang et al., 2024c, 2024d), applied to balance competing objectives such as performance and cost. Studies indicate that MOO optimization significantly enhances the performance and energy generation of multi-generation systems for cooling, heating, and power while maintaining cost-effectiveness (Sami et al., 2024; Mobayen et al., 2025; Alirahmi and Assareh, 2020). To further refine system design and improve efficiency, energy simulations have also been conducted to evaluate system performance under varying climatic and operational conditions (Sami et al., 2024; Nikitin et al., 2023; Buonomano et al., 2023), demonstrating the practicality and modularity of these systems.

MOO strategies have been integrated with simulation software such as EnergyPlus for detailed building energy performance simulations, TRNSYS for transient system modeling, and Building Energy Optimization (BEopt) for optimizing energy-efficient building designs (Tajalli-Ardekani et al., 2024; Melo et al., 2021; Tool, 2024). These studies highlight the role of TRNSYS in supporting urban energy transitions, EnergyPlus in enhancing energy supply strategies for high-rise buildings, and BEopt in refining net-zero building designs through precise energy modeling. The results further indicate that integrating MOO techniques with these tools has led to a 68.2 % reduction in purchased electricity, a 56 % decrease in CO<sub>2</sub> emissions, and a 48.9 % cut in generation costs while optimizing energy supply strategies and enhancing the sustainability of net-zero buildings. Among the various optimization tools, BEopt has been extensively applied in optimizing ZEBs by integrating renewable energy sources, offering a robust framework for

evaluating building energy performance under varying conditions (Rhodes et al., 2015; Christensen et al., 2005, 2006; Assareh et al., 2024a). Similarly, Engineering Equation Solver (EES) is widely used for solving complex thermodynamic equations in multi-functional energy systems, making it relevant for solar-driven multi-generation applications (Assareh et al., 2025a; Adib et al., 2023; Zhang et al., 2024b). Beyond these tools, MOO techniques such as Response Surface Methodology (RSM) have been utilized to optimize key performance objectives, including maximizing exergy efficiency while minimizing costs (Bellos and Tzivanidis, 2019; Assareh et al., 2024b). While these optimization methods have significantly improved the reliability and cost-effectiveness of solar-powered energy systems (Auza et al., 2024; Li et al., 2023; Abdou et al., 2021), their application has been largely limited to small-scale buildings (Sarvar-Ardeh et al., 2024; Mohtasim et al., 2025), overlooking their potential for large-scale, multi-functional structures with complex and high energy demands, such as university campuses.

University buildings require a continuous and dynamic energy supply to support diverse functions, such as laboratories, offices, and other high-demand facilities (Lykas et al., 2023; Zhang et al., 2024a). These buildings also face significant daily and seasonal energy demand fluctuations, especially in severe climates where energy consumption is exceptionally high. These fluctuations, coupled with the scale and complexity of university operations, present unique challenges for integrating renewable energy sources effectively. While the advantages of multi-generation systems with renewable energy sources for residential and small commercial buildings are well-documented, their application in large academic institutions, where energy demands are more extensive and variable, remains insufficiently explored (Sretenovic, 2013; Zhao et al., 2024; Gjoka et al., 2024). This challenge is intensified by the tight budget constraints of university campuses, which necessitate balancing technical efficiency and economic feasibility for the long-term adoption of solar-powered multi-generation systems (Lykas et al., 2023; Buonomano et al., 2023; Gjoka et al., 2024). Addressing this research gap, this study designs and optimizes a solar-powered multi-generation system for a university building in Dezful, Iran, a cooling-dominant location with an extremely hot climate. The study introduces a novel framework combining machine learning-based MOO and simulation tools to optimize energy systems by maximizing efficiency, minimizing costs, and generating surplus energy. RSM is positioned as a lightweight supervised machine learning technique that efficiently models and optimizes input-output relationships, serving as a computationally efficient and interpretable link between statistical methods and modern ML approaches. This paper is structured as follows: Section 2 details the methodology, including modeling and optimization using BEopt, EES, and RSM; Section 3 focuses on system design and analysis; Section 4 presents the results and discussion; Section 5 addresses the limitations and future work; and Section 6 concludes the study with key findings and implications.

## 2. Methodology

This section outlines the utilized methodology in this study, comprising two main stages: 1- System Analysis and Design and 2- Optimization and Performance Evaluation. These stages ensure a precise framework for designing, modeling, and optimizing a solar-powered multi-generation system for large-scale applications. The methodology involves the following.

**1 System Analysis and Design:** This stage focuses on selecting and analyzing the case study building, collecting relevant data, and simulating the energy demands to provide baseline inputs for the proposed system. It includes:

✓ **Case Study Selection:** The Engineering and Technology Faculty building at the Islamic Azad University of Dezful (IAUD) in Dezful,

Iran, was selected due to its high cooling demand and solar energy potential.

- ✓ **Data Collection:** Details about the building's dimensions, layout, material composition, and energy demands were collected, along with climatic data (e.g., solar irradiance, temperature, wind speed) obtained using Meteonom software.
  - ✓ **Energy Load Simulation and Analysis:** BEopt software was employed to simulate the building's annual energy demands and assess the impact of materials and design, providing baseline input data for the system configuration.
- 2 **Optimization and Performance Evaluation:** This stage focuses on designing and modeling the multi-generation system, optimizing its performance, and evaluating its outputs. It includes:
- ✓ **System Design and Modeling:** Thermodynamic analysis was conducted using EES to evaluate energy outputs (electricity, heating, and cooling) and assess exergy efficiency.
  - ✓ **Multi-Objective Optimization (MOO):** RSM, framed as a light-weight supervised machine learning technique, was utilized to optimize critical design variables, such as PV panel dimensions, to maximize exergy efficiency and minimize operational costs. By leveraging labeled input-output data, RSM efficiently models and optimizes relationships between variables while maintaining interpretability. Compared to artificial intelligence approaches such as GAs, which are computationally intensive, and ANNs, which require extensive training and are less transparent, RSM offers simplicity, computational efficiency, and reliability. These attributes make it ideal for moderately complex applications like the proposed solar farm (Pereira et al., 2022; Susaimanickam et al., 2023).
  - ✓ **Performance Outputs and Benchmarking:** The optimized system's performance was evaluated in terms of efficiency, operational cost, and CO<sub>2</sub> emission reduction. The results were

benchmarked against existing systems to validate the proposed design's effectiveness.

- ✓ **Final Design and Validation:** The system's performance metrics were refined and validated through iterative analysis to ensure alignment with the study's objectives.

A schematic representation of the methodology is presented in Fig. 1, summarizing the steps involved in the analysis, optimization, and validation of the proposed system.

### 3. System design and analysis

This section outlines the first stage of the methodology, focusing on analyzing the case study building, collecting relevant data, and simulating its energy demands to establish baseline inputs for the proposed solar-powered multi-generation system.

#### 3.1. Case study description and Data Collection

The case study, Engineering and Technology Faculty Building at IAUD, located in Dezful, Iran. This case was selected to investigate energy-efficient solutions for a large, multifunctional facility operating in an extreme climate. Dezful, situated in the southwestern Khuzestan Province, is highlighted in Fig. 2. The region's climate, classified as hot semi-arid (BSh) under the Köppen system, features prolonged, scorching, and dry summers with short, mild winters and minimal rainfall. Such environmental conditions result in substantial energy requirements, particularly for cooling during the warmer periods, making this building an ideal example for evaluating advanced energy systems.

The case study building is a three-floor educational facility designed to support academic and administrative functions. Fig. 3 presents the exterior view of the case study building, showcasing its architectural design, and three floors layout.

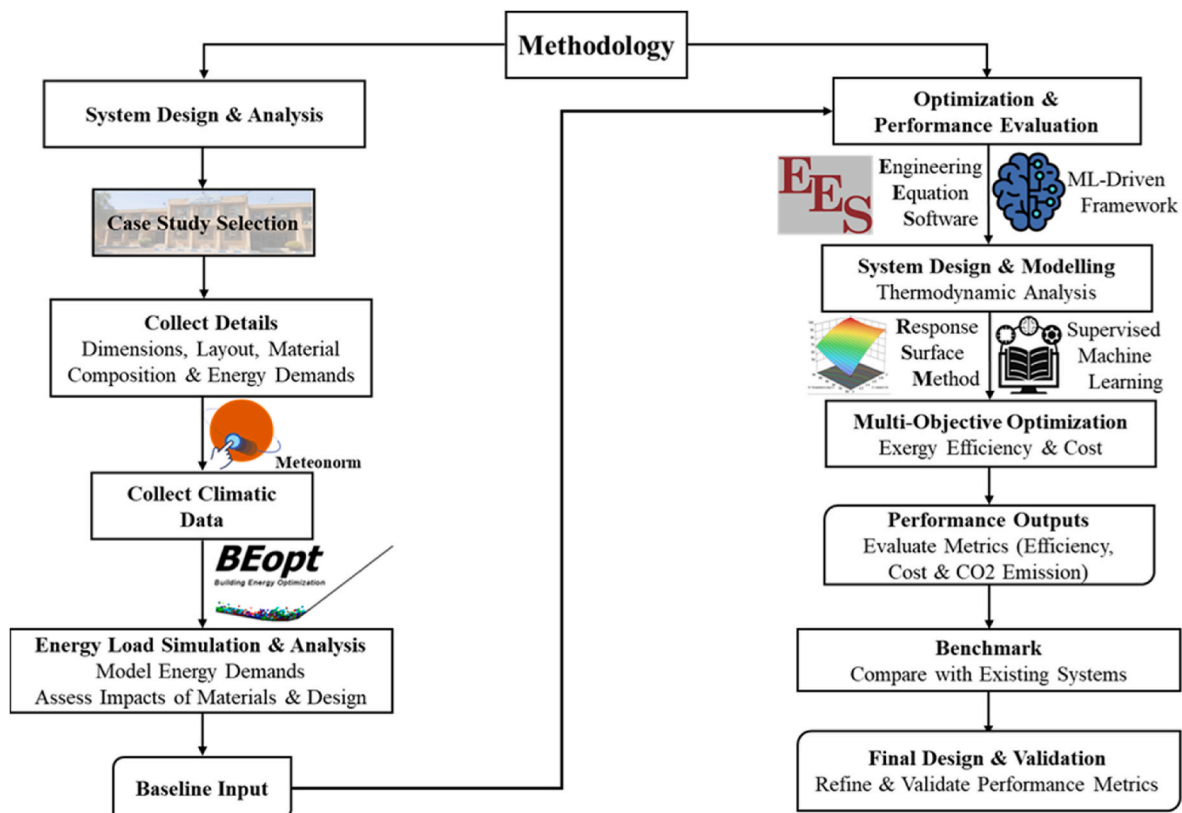


Fig. 1. Methodology framework for system design and optimization.

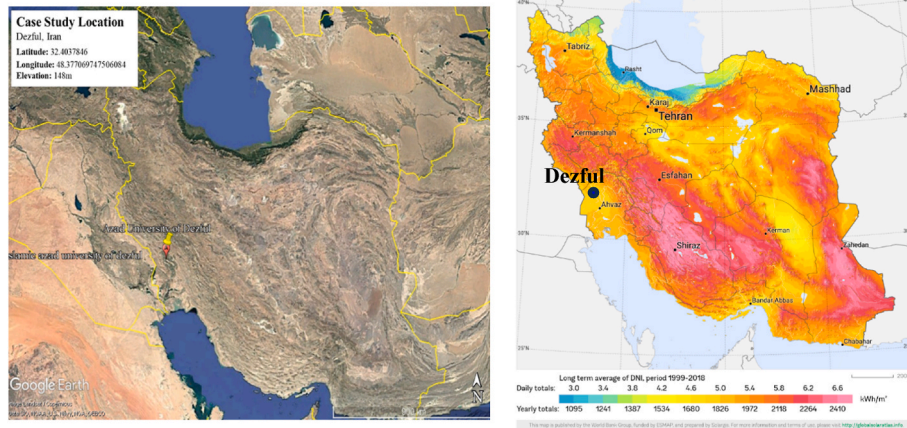


Fig. 2. Case study location (GoogleEarth, 2025) and solar energy Map (ESMAP and Energy Sector Management Assistance Program, 2024).

Table 1 provides an overview of the sizes and construction details of the case study building, which consists of three floors. It includes the dimensions of each floor, and the construction materials used. The materials vary across the floors to address specific functional needs, structural requirements, and energy efficiency objectives.

BEopt is used to model energy demand based on inputs such as building details, construction materials, and climatic data. It simplifies energy modeling with its user-friendly interface and robust optimization engine, systematically evaluating various design configurations to calculate annual energy loads, including cooling, heating, and power requirements (Tool, 2024; Barber and Krarti, 2022). By analyzing critical aspects of the building, such as the envelope and insulation, BEopt provides accurate energy demand simulations, which serve as a baseline dataset for configuring the proposed multi-generation solar-powered system. This dataset is subsequently leveraged in the machine learning-driven optimization framework, where RSM uses these labeled input-output relationships to optimize system performance.

BEopt is particularly effective for modeling energy performance in multifunctional buildings like university campuses, where diverse energy requirements must be considered (Assareh et al., 2025a; Mobayen et al., 2025). While alternative software, such as TRNSYS Type 56, could provide transient simulations and detailed dynamic analyses, BEopt was selected for its suitability in assessing annual energy demands under steady-state conditions. This aligns with the study's approach to generating baseline inputs for the ML-driven optimization process, enhancing computational efficiency and interpretability. Fig. 4 illustrates the process of defining building parameters, inputting climatic data, running simulations, and providing baseline energy demands using BEopt as inputs for system optimization.

Fig. 5 illustrates the annual hourly variations of key environmental parameters, including global horizontal and diffuse solar irradiance, ambient temperature, dew point, relative humidity, and wind speed, for the case study location, Dezful, Iran. Global horizontal irradiance (GHI) represents the total solar energy received on a horizontal surface, while diffuse irradiance accounts for scattered sunlight reaching the surface. The data highlights significant solar energy potential, with irradiance reaching up to  $1000 \text{ W/m}^2$  during peak hours, particularly in the summer months, making Dezful ideal for solar energy systems. Ambient temperature varies seasonally, peaking between April and September, with values reaching up to  $60^\circ\text{C}$ , while cooler periods in December and January see temperatures drop closer to  $0^\circ\text{C}$ . Dew points fluctuate between  $-5^\circ\text{C}$  in cooler months and  $25^\circ\text{C}$  in summer, reflecting seasonal changes in moisture content, which influences indoor comfort and cooling requirements. Relative humidity ranges from near 0 % during hot, dry summer months to 100 % during cooler, wetter periods, further emphasizing seasonal variability. Wind speeds vary from 0 to 16 m/s throughout the year, with higher values typically observed during

transitional seasons, offering potential for wind energy integration. Notably, higher wind speeds tend to coincide with lower relative humidity levels, particularly during dry seasons, suggesting the potential role of wind in dispersing moisture and creating drier air conditions. These variations highlight the region's extreme climate, its high cooling demand during summer, and its suitability for renewable energy systems, providing critical baseline inputs for optimizing the proposed solar-powered multi-generation system to enhance energy efficiency and sustainability.

Fig. 6 indicates the temperature profile within the case study building, showing annual variations in indoor living space temperatures and their alignment with the defined heating and cooling set points, which maintain an ideal range between  $21^\circ\text{C}$  and  $25.5^\circ\text{C}$ . During colder months, heating set points prevent temperatures from dropping below  $21^\circ\text{C}$ , while cooling set points ensure temperatures do not exceed  $25.5^\circ\text{C}$  during warmer months. This balance reflects the integration of energy management strategies aimed at optimizing thermal comfort and minimizing energy consumption. Maintaining a stable indoor environment is a key point for enhancing occupant well-being, productivity, and cognitive performance, particularly in educational facilities. The figure highlights the system's ability to effectively manage heating and cooling loads, contributing to reduced energy use and operational costs, aligning with the study's objectives of achieving energy efficiency and sustainability in high-demand environments.

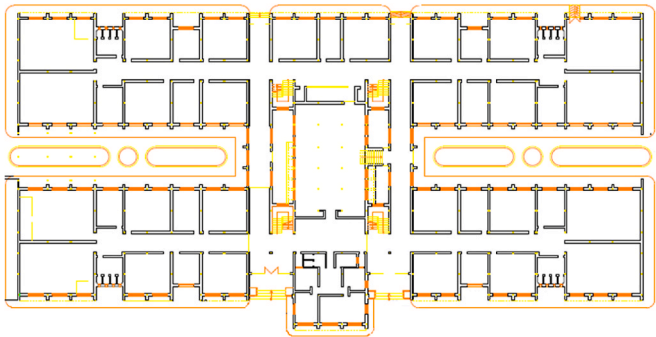
This section presents the energy consumption analysis for the case study. Fig. 7 illustrates the hourly energy consumption patterns for cooling, heating, lighting, and total electricity throughout the year in the case study. Cooling is the dominant energy demand, peaking at 3500 kWh during the summer months (June to August), while heating demand is negligible, reaching only 110 kWh during winter mornings. Lighting demand remains steady year-round, with peaks up to 3000 kWh during evening hours. Total electricity usage fluctuates between 0 and 5500 kWh, with seasonal peaks in summer driven by cooling needs and smaller spikes in winter for heating. This analysis highlights seasonal variations and the substantial role of cooling in the building's energy consumption.

Fig. 8 provides a thermal contour visualization of the hourly energy consumption patterns, showcasing the dominance of cooling loads in summer and the negligible heating requirements in winter. It highlights how energy demand for cooling, lighting, and total electricity varies throughout the day and across seasons, emphasizing cooling's midday peaks during summer. The contours also illustrate the stable lighting demand and minimal heating, reinforcing the need for targeted cooling strategies to enhance energy efficiency. By offering a clear visual representation, the figure complements the numerical analysis from Fig. 7 and supports the study's focus on sustainable energy management.

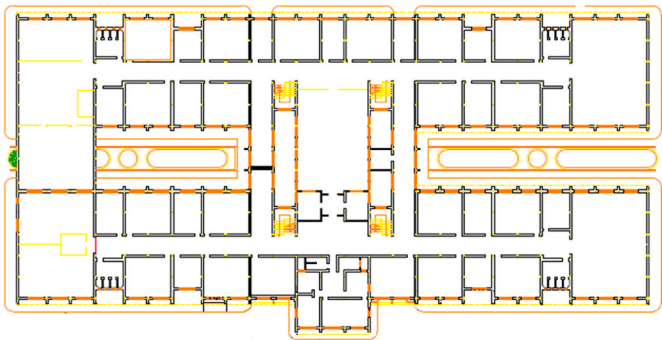
Table 2 highlights the annual energy usage breakdown in the case



Floor 1



Floor 2



Floor 3

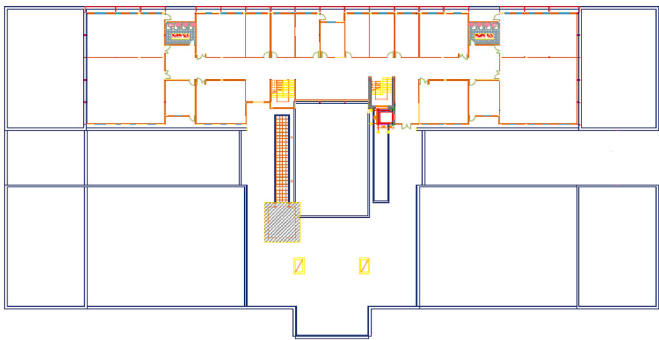


Fig. 3. Exterior view and floor layout of the case study building.

study, emphasizing the dominance of cooling, which accounts for approximately 41 % of total electricity consumption. Cooling demand is more than 1000 times greater than heating and around 21 % higher than lighting, reflecting its significant role in the building's energy profile. Lighting contributes roughly 34 % of total electricity consumption, while heating is negligible at less than 1 %. This analysis underscores the critical need to optimize cooling and lighting systems, as they together constitute the majority of electricity usage, to enhance energy efficiency

and sustainability.

Table 3 provides insights into the case study building's financial, energy, and environmental impacts. The life cycle and annualized costs highlight the significant economic implications of meeting the building's energy demands, emphasizing the importance of cost-efficient energy strategies. The site energy consumption indicates high energy dependency, particularly due to cooling and lighting needs in Dezful's hot climate. The CO<sub>2</sub> emissions, while moderate, reflect the building's

**Table 1**  
Dimensions and construction materials of the case study building.

| Information                           | Unit           | Value |
|---------------------------------------|----------------|-------|
| Ground and First Floor Length         | m              | 110   |
| Ground and First Floor Width          | m              | 51    |
| Ground and First Floor Infrastructure | m <sup>2</sup> | 5670  |
| Second Floor Length                   | m              | 80    |
| First Floor Width                     | m              | 20    |
| Second Floor infrastructure           | m <sup>2</sup> | 1600  |
| Number of Floors                      | –              | 3     |

| Floor Number           | Component      | Material                                |
|------------------------|----------------|---|
| First and Second Floor | Windows        | Metal                                   |
|                        | Interior Doors | Wooden                                  |
|                        | Outer Doors    | Metal                                   |
|                        | Internal Walls | Brick                                   |
|                        | Facade Walls   | 3 cm Brick                              |
|                        | Floor Material | Mosaic                                  |
|                        | Skeleton       | Metal                                   |
| Third Floor            | Roof           | Plaster                                 |
|                        | Windows        | Unplasticized Polyvinyl Chloride (UPVC) |
|                        | Interior Doors | Wooden                                  |
|                        | Outer Doors    | Stramit                                 |
|                        | Internal Walls | Brick                                   |
|                        | Facade Walls   | 3 cm Brick                              |
|                        | Floor Material | Ceramics                                |
|                        | Skeleton       | Light metal                             |
|                        | Roof           | Plaster                                 |

reliance on conventional energy sources, underscoring the potential for renewable energy integration to considerably reduce both environmental impact and operational costs. Together, these metrics highlight the critical need for sustainable and energy-efficient solutions to enhance the building's economic and environmental performance.

### 3.2. Solar farm configuration and system setup

The solar farm's configuration, its energy generation capabilities, and the employed performance optimization strategies are presented in this section. The following sections will detail the system's technical setup, including the PV panels and their integration with cooling and heating systems, as well as the methodologies used for optimizing both exergy efficiency and cost-effectiveness.

#### 3.2.1. Solar farm design

Fig. 9 illustrates the schematic design of the proposed solar farm, which integrates PV panels with a condensing chiller unit to meet the building's cooling, heating, and electricity demands. The PV panels capture solar energy and generate electricity, which powers the system components, including a compressor, condenser, and evaporator. The compressor facilitates heat exchange, the condenser provides heating energy, and the evaporator supplies cooling energy to maintain indoor thermal comfort. This integrated design ensures efficient energy utilization for multiple functions while reducing dependency on external

power sources and minimizing carbon emissions.

Fig. 10 shows key steps in the methodology, integrating a machine learning-driven optimization framework. The process begins with the collection of weather data, including solar energy and ambient temperature, through Meteotest (Meteotest) for accurate climate simulation. The system's components, such as PV panels and a compression chiller, are modeled to align with energy requirements, while thermodynamic and economic analyses are conducted using EES software to evaluate energy, exergy, and economic metrics. MOO is performed using RSM, framed as a lightweight supervised machine learning technique. By leveraging labeled input-output data, such as climatic conditions and energy performance metrics, through Design-Expert or Design of Experiments (DOE) software (Stat-Ease, 2021), RSM efficiently models and optimizes the system to achieve two objectives: maximizing exergy efficiency (%) and minimizing the cost rate (\$/h). This methodology, adopted for Dezful, Iran, takes advantage of its high solar energy potential to provide sustainable energy solutions while ensuring computational efficiency, interpretability, and scalability within the broader ML framework.

This study employs the RSM, framed as a lightweight supervised machine learning technique, to optimize the suggested system performance, as illustrated in Fig. 11. The process begins with defining key independent variables and their ranges, which serve as labeled input data for the supervised learning process. Experiments are designed using the Central Composite Design (CCD) within the Design of Experiments (DOE) framework (Allaix and Carbone, 2011; Li et al., 2016), ensuring an efficient exploration of the input-output relationships. Simulation analysis is conducted to evaluate system performance, and statistical analysis, including Analysis of Variance (ANOVA), is used to assess the model's accuracy, validity, and reliability. Once the model satisfies the required standards, it determines optimal values that maximize performance metrics, leveraging the interpretable and computationally efficient nature of RSM within the broader machine learning-driven optimization framework. This systematic approach ensures the development of a valid, reliable, and interpretable model for multi-objective optimization.

#### 3.2.2. Thermodynamic analysis and assumptions

Mass and energy balances are computed for each control volume as part of the thermodynamic analysis. To simplify, several assumptions are applied.

- 1 Steady-state conditions: All processes are assumed to occur under steady-state conditions, where system variables such as pressure, temperature, and flow rates remain constant over time. This assumption simplifies the analysis by eliminating the need to model transient dynamics and aligns with the paper's focus on long-term performance.
- 2 Negligible pressure drops in pipelines: Pressure drop analysis in pipelines is not explicitly modeled, and it is assumed that pressure drops are negligible. This simplifies calculations and computational

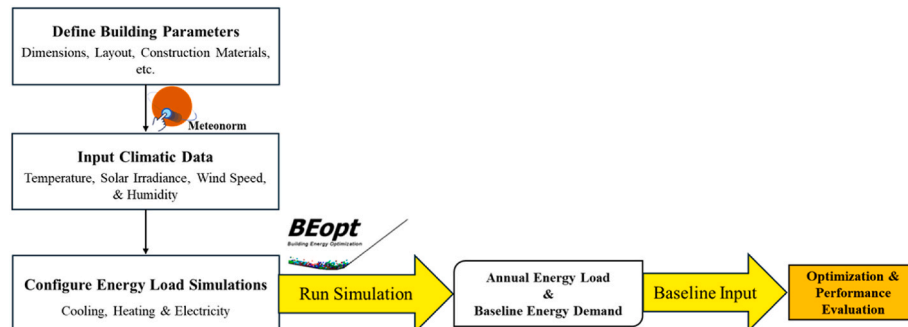


**Fig. 4.** BEopt process for generating baseline inputs for optimization.

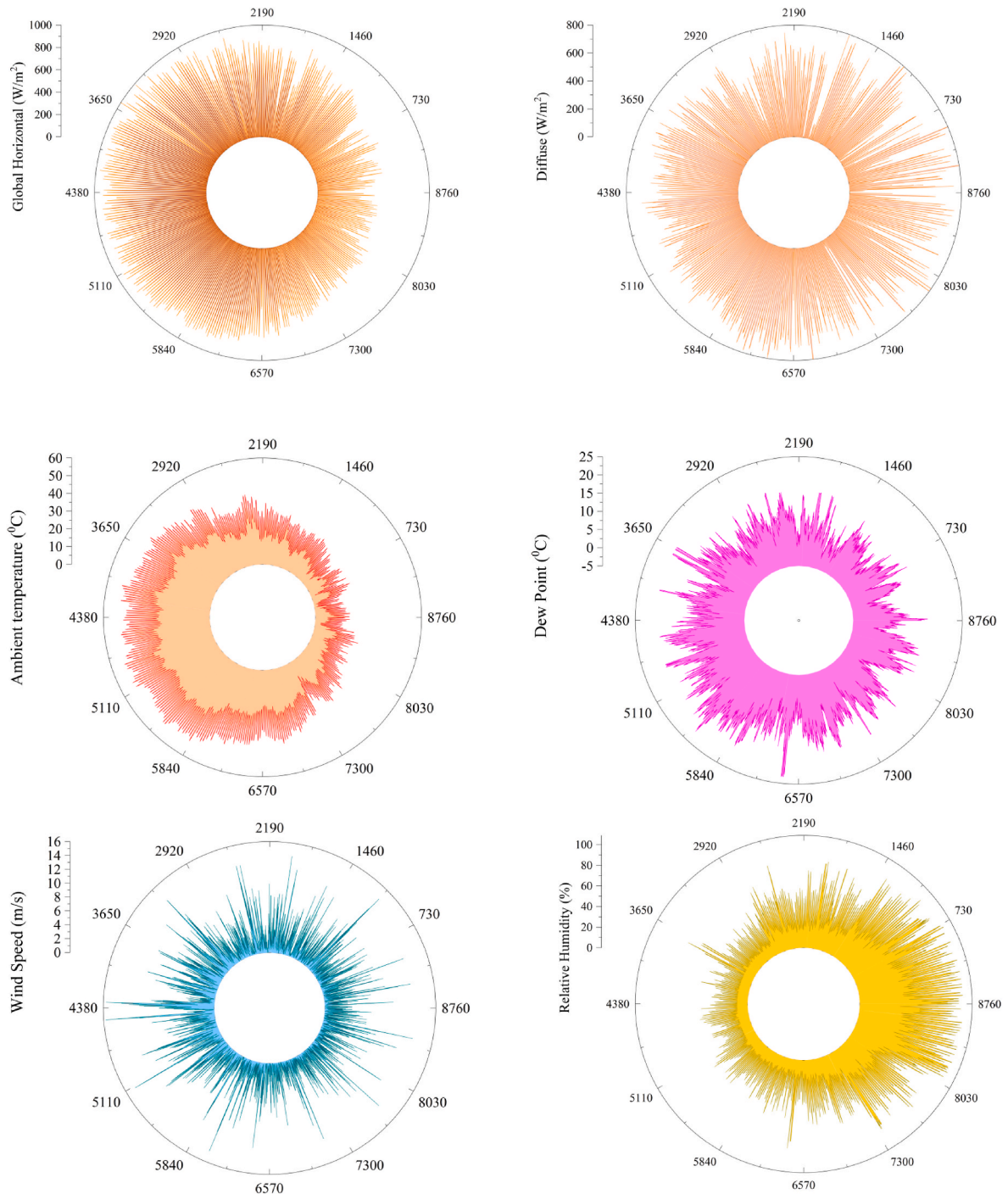


**Fig. 5.** Annual hourly variations of Dezful's climate parameters.

requirements, which is consistent with the study's streamlined thermodynamic modeling approach.

3 Insignificant potential energy changes: Changes in potential energy are assumed to be negligible compared to thermal and mechanical energy changes. This is reasonable given the system's flat terrain and absence of significant elevation differences. This assumption minimizes complexity in the labeled dataset, improving the interpretability of the supervised learning model

4 Insignificant kinetic energy changes: The model assumes that kinetic energy changes are negligible relative to thermal and mechanical energy. This assumption is valid for systems with moderate flow velocities, as the manuscript does not emphasize high-speed flow

scenarios. By excluding kinetic energy changes, the dataset remains streamlined, enhancing the supervised learning model's ability to capture key relationships without being influenced by minor variables.

The analysis relies on basic thermodynamic principles, with functional relationships referenced from sources (Li et al., 2016; Mehrpooya et al., 2021; Delpisheh et al., 2021; Din et al., 2017). Table 4 outlines the input data used for the solar farm analysis.

In this analysis, the thermodynamic values for the refrigeration cycle, including enthalpy and entropy changes, were computed using EES. The cycle employs R-134a as the working fluid, chosen for its

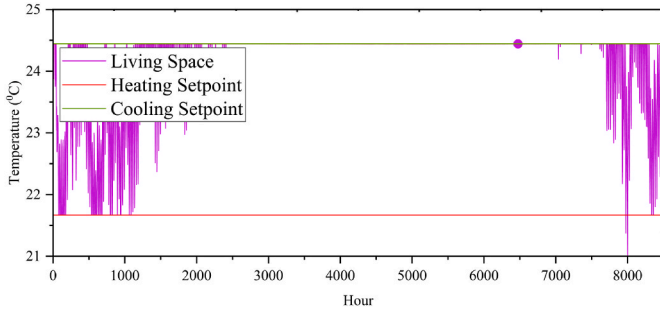


Fig. 6. Temperature profile and heating/cooling adjustments in the case study.

efficiency and compatibility with the solar-powered system's temperature range. The heat is harnessed from the cycle's condenser, contributing to the system's integrated heating capabilities. Detailed thermodynamic properties are outlined in Appendix A to support transparency in the calculations.

To assess the system's performance, Equations (1)–(3) calculate the PV panel's electrical output, whereas Equations (4) and (5) determine the thermal output parameters. Although these equations might resemble those used in a Photovoltaic Thermal (PVT) collector, this system independently evaluates electrical and thermal components. Each equation has been selected to capture relevant output factors, providing a clear basis for optimizing both energy and exergy efficiency within this multi-generation solar farm. Exergy efficiency is defined as the measure of a system's ability to convert available energy into useful work by accounting for both energy quality and quantity. For a multi-generation system producing electricity, heating, and cooling, exergy efficiency provides a comprehensive metric to evaluate performance by capturing the thermodynamic quality of each energy form. This approach allows for a nuanced analysis of energy use, making it particularly effective for optimizing complex systems like the solar-powered multi-generation setup in this study. Specifically, Equation (1) represents the application of the first law of thermodynamics for each control volume.

$$\Delta E = \dot{Q} - \dot{W} + \sum \dot{m} \times h = \dot{Q} - \dot{W} + \sum_i \dot{m}_i \left( h_i + \frac{v_i^2}{2} + gZ_i \right) - \sum_e \dot{m}_e \left( h_e + \frac{v_e^2}{2} + gZ_e \right) = \frac{dE_{cv}}{dt} \quad (1)$$

$\Delta E$  is the change in total energy (internal, kinetic, potential) of the system.  $\dot{Q}$  and  $\dot{W}$  represent the rate of heat and work transfer,  $\dot{m}$  is the mass flow rate, and  $h$  is the specific enthalpy of the incoming or outgoing fluid.

### 3.2.3. Performance metrics and efficiency calculations

Using Equation (2), the useful energy produced by the PV panel is calculated:

$$\dot{Q}_{PV} = ((\dot{m}_{air} \times C_{air}) / U_l) \times (h_{p2g} \times Z \times GB) - (U_l \times (T_{air,in} - T_0)) \times (1 - \exp((-b \times U_l \times L) / \dot{m}_{air} \times C_{air})) \quad (2)$$

The production power of the PV panel is calculated from Equation (3):

$$W_{PV} = \eta_{PV} \times A_{PV} \times G \quad (3)$$

The electrical power output or production power of the PV panel ( $W_{PV}$ ), measured in watts (W), represents generated electrical power.

The conversion efficiency ( $\eta_{PV}$ ) represents how efficiently the panel converts sunlight into electricity. Higher efficiency means that more of the solar energy is turned into electrical energy.  $A_{PV}$  is the area of the PV panel (in square meters,  $m^2$ ) and  $G$  is solar irradiance or solar power incident on the panel (in watts per square meter,  $W/m^2$ ).

Solar panel thermal efficiency is calculated using Equation (4):

$$\eta_{thermal} = \frac{\dot{Q}_{useful}}{A_{PV} \times G} \quad (4)$$

In this equation,  $\eta_{thermal}$  is the thermal efficiency of the solar panel,  $\dot{Q}_{useful}$  is the useful heat output or the collected thermal energy (in watts, W), The area of the PV panel is simply determined by multiplying Width (b) and Length (L), as shown in Equation (5).

$$A_{PV} = b \times L \quad (5)$$

## 4. Results and discussion

The findings in this study reveal the system's applicability to high-demand environments like university campuses, particularly those in severe hot climates. This section presents the solar farm's performance results and optimization. Advanced techniques were used to improve technical efficiency and economic feasibility, enhancing energy generation, reducing costs, and boosting sustainability. By framing RSM as a lightweight supervised machine learning technique, this study demonstrates how labeled input-output data (e.g., PV parameters and performance metrics) can be leveraged for efficient and interpretable optimization. The next subsection details the MOO process for optimizing exergy efficiency and cost-effectiveness.

### 4.1. Multi-objective optimization

The MOO process was conducted using RSM within a machine learning-driven framework to maximize the exergy efficiency and minimize the system cost rate. Table 5 outlines three input factors along with their respective ranges.

The selected input parameters were chosen based on their substantial influence on both MOO's objectives. These parameters were identified as the most significant factors affecting the MOO goals through preliminary analyses, directly and considerably impacting the system's performance and cost-effectiveness. By focusing on these key parameters, we ensured that the optimization would target the factors with the greatest potential for improvement in energy and cost performance. The supervised learning approach inherent in RSM facilitates this by efficiently modeling and optimizing the relationships between input parameters and system performance metrics.

In this study, the concept of "desirability" refers to a combined measure used in the MOO to assess how well a particular solution meets each of the targeted objectives: exergy efficiency and cost rate. Desirability ranges from 0 (least desirable) to 1 (most desirable), representing an ideal balance between objectives. Here, the RSM generates multiple solutions with varying levels of desirability, allowing for an optimized

selection based on the best balance between energy efficiency and cost-effectiveness. This approach is particularly useful in multi-objective scenarios, where improving one objective can sometimes adversely affect another. RSM's role as a lightweight supervised machine learning technique ensures that complex interactions between variables are captured and optimized effectively, providing interpretable solutions for multi-objective challenges.

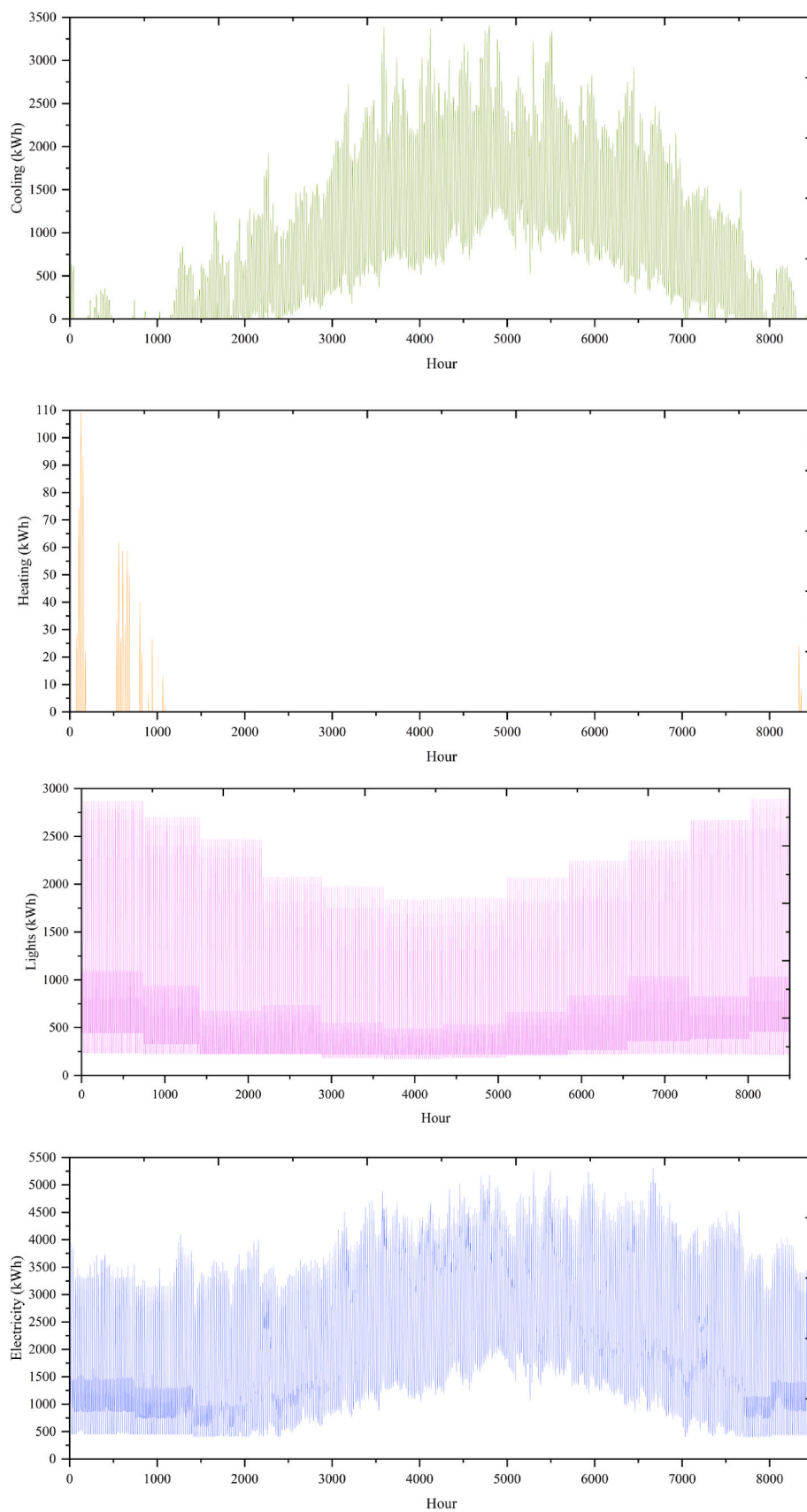


**Fig. 7.** Annual hourly variations of cooling, heating, and lighting electricity usage in the case study.

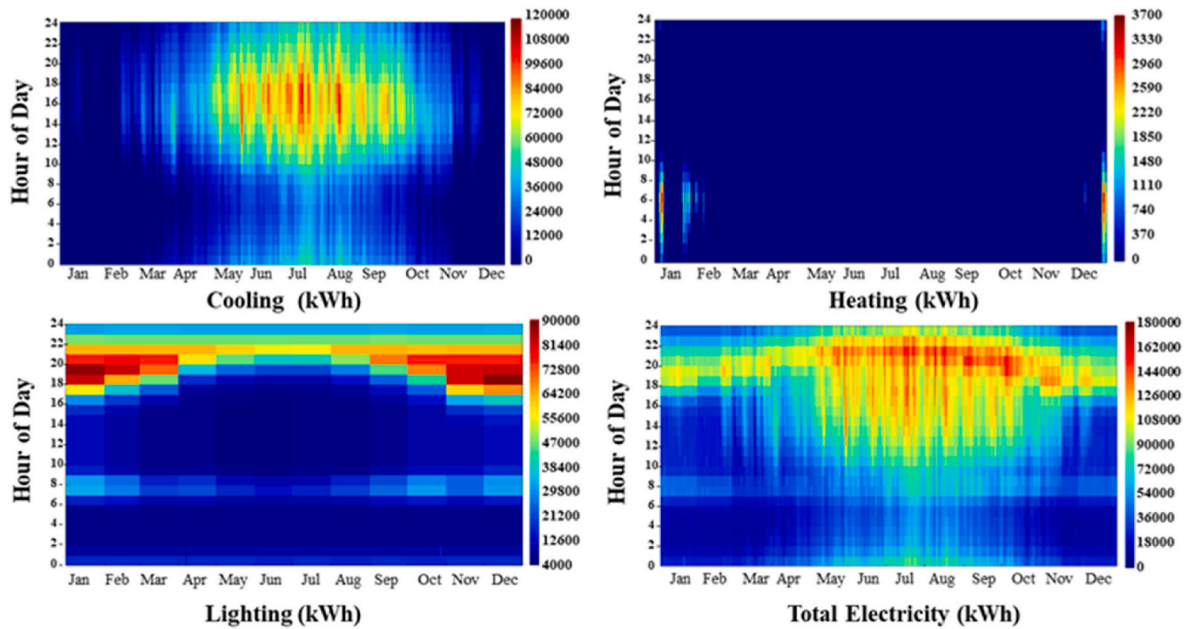


Fig. 8. Thermal contours representing hourly energy usage for the case study.

**Table 2**

Annual energy breakdown: Cooling, heating, and lighting.

| Energy Consumption | Unit | Amount     |
|--------------------|------|------------|
| Cooling            | kWh  | 7,517,611  |
| Heating            | kWh  | 6571.734   |
| Lights             | kWh  | 6,226,048  |
| Total Electricity  | kWh  | 18,238,280 |

**Table 3**

Costs, energy use, and emissions amount.

| Parameter                             | Unit                                     | Amount       |
|---------------------------------------|--|--------------|
| Energy Related Costs, Life Cycle Cost | \$                                       | 224,315.6406 |
| Energy Related Costs, Annualized      | \$/yr                                    | 6478.200195  |
| Site Energy Consumption               | Million British Thermal Units (MMBtu)/yr | 193.3800049  |
| CO <sub>2</sub> Emissions             | Metric tons/yr                           | 37.18        |

While EES includes built-in optimization methods, the RSM approach was chosen because it offers flexibility in MOO and is particularly well-suited for exploring complex interactions between variables. The RSM technique allows us to optimize both technical (exergy efficiency) and economic (cost rate) objectives simultaneously, which aligns with the study's goal to enhance system performance holistically. Furthermore, RSM enables the generation of response surfaces that can provide a clear visual representation of optimal performance regions, aiding in decision-making for large-scale system implementations.

The outcomes from the 25 required runs were analyzed using RSM and DOE software to enhance the solar farm's performance and identify the optimal values for the objective functions. This study leverages advanced RSM techniques within the context of supervised learning to simultaneously optimize exergy efficiency and cost rate, an approach that uniquely considers both the technical and economic viability essential for scaling such systems to large educational buildings with complex energy needs. The MOO methods applied here provide a comprehensive framework adaptable to other large-scale facilities. The appendix contains the outcomes for 100 optimized points using RSM. Table 6 presents the most optimal solution for both the decision

variables and objective functions, following a detailed review of the MOO method used in this study.

In this study, exergy efficiency is computed by assessing the individual exergies of cooling, heating, and electricity, and then comparing these outputs to the total exergy input from solar radiation. This method ensures that each output type's thermodynamic quality is considered, thus providing a clearer understanding of where energy quality is lost across the system. Such an analysis is essential for systems that serve multiple functions, as it highlights areas for further optimization to enhance both energy and exergy efficiency.

Fig. 12 shows the impact of three input variables, the number, width, and length of the PV panels, on exergy efficiency. The contour plots indicate that the number of PV panels has the most significant influence, with efficiency increasing steeply as the number rises from 90 to 130. In contrast, increasing the width and length of the panels shows a more moderate impact, with efficiency improvements stabilizing beyond approximately 1.44 m<sup>2</sup> for width and 3.63 m<sup>2</sup> for length. The optimal exergy efficiency of 25.69 % is achieved with 130 panels, a width of 1.44 m<sup>2</sup>, and a length of 3.63 m<sup>2</sup>. While this figure highlights the importance of optimizing these parameters for efficiency, it is also critical to evaluate their impact on cost, which will be addressed in the next figure. The red zones highlight the optimal design space, emphasizing the need to balance efficiency and cost for a practical and sustainable solar farm configuration.

Fig. 13 depicts the simultaneous impacts of input variables on the suggested solar farm cost rate, with red areas indicating higher costs and green areas showing lower costs. The results reveal that the number of PV panels has the most significant effect on reducing costs, with the cost rate declining sharply as the number increases from 90 to 130. In comparison, the width and length of the panels have a more moderate influence, with cost reductions stabilizing beyond 1.44 m<sup>2</sup> for width and 3.63 m<sup>2</sup> for length. The optimal configuration, achieving a cost rate of \$10.15/hour, involves 130 PV panels with these dimensions. This analysis, combined with the impacts of these inputs on exergy efficiency, suggests that balancing a higher number of panels with moderate panel dimensions (width and length) yields both lower costs and improved efficiency. Such a configuration maximizes energy generation while maintaining cost-effectiveness, providing insights for designing economically viable and high-performing solar farms.

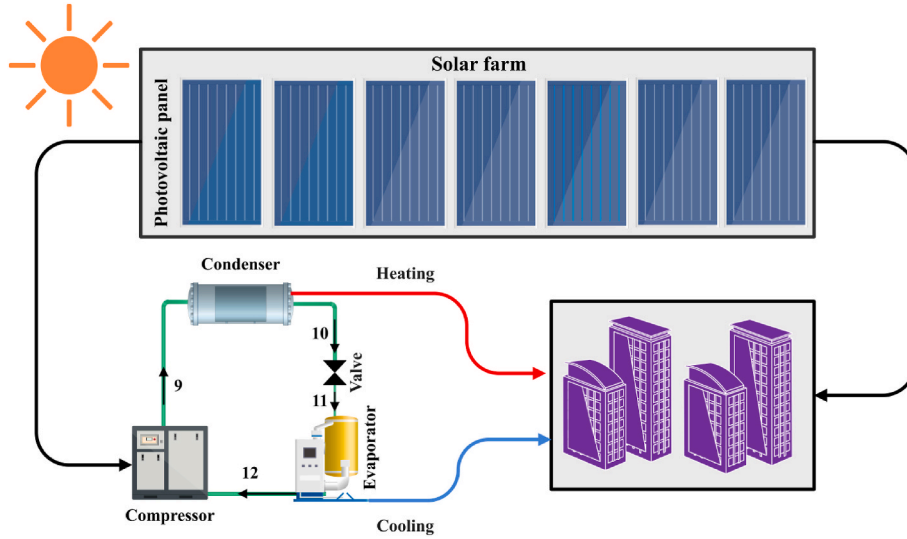


Fig. 9. Schematic design of the proposed solar farm.

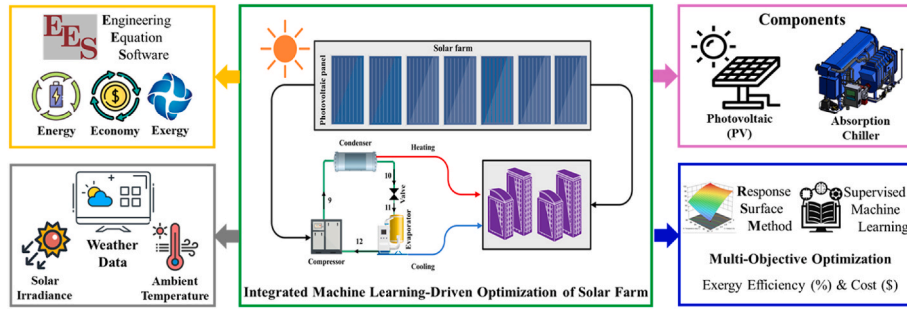


Fig. 10. Solar farm modeling methodology.

#### 4.2. Exergy analysis of system components

Fig. 14 shows the total exergy destruction rate of 3246.00 kWh and highlights the contributions from key components of the system. The compression chiller is responsible for the largest share of exergy destruction, consuming 3130 kWh, which indicates significant energy losses during its operation. In contrast, heating contributes 1975 kWh to exergy destruction, while cooling accounts for a relatively smaller amount of 1523 kWh. The solar farm generates 14456 kWh, with energy losses distributed across these components, highlighting the need for targeted improvements in the compression chiller and heating systems to enhance efficiency. In this case, the high exergy destruction in the compression chiller suggests that its energy-intensive processes, such as heat exchange and compression, are critical bottlenecks in the system's performance.

#### 4.3. Economic analysis

The cost equation for the system was developed by calculating the operational costs of each component, including both the solar PV panels and the compression chiller. The total cost rate (\$/h) is derived by considering the power input, maintenance, and component depreciation. Each cost component was assessed individually to ensure precise allocation, allowing for optimized system-level cost analysis. For this purpose, the cost rate was measured using Equation (6) (Sullivan et al., 2015):

$$\text{Cost Rate} = \text{Cost}_{\text{Operation}} + \text{Cost}_{\text{Maintenance}} + \text{Cost}_{\text{Depreciation}} \quad (6)$$

$$\text{Cost}_{\text{Operation}} = P_{\text{input}} \times t \times \text{Cost}_{\text{electricity}}$$

$$\text{Cost}_{\text{Maintenance}} = \frac{\text{Cost}_{\text{Component}} \times m_{\text{Rate}}}{L_{\text{Component}}}$$

$$\text{Cost}_{\text{Depreciation}} = \frac{\text{Cost}_{\text{Component}}}{L_{\text{Component}}}$$

$P_{\text{input}}$  is the required power by component,  $t$  is the operating time,  $m_{\text{Rate}}$  represents the annual maintenance rate (percentage of the initial cost), and  $L_{\text{Component}}$  is the lifespan of the component (years).

Fig. 15 illustrates the total cost rate of the system alongside its primary components, categorized into the solar farm and the compression chiller. The total cost rate is \$10.305 per hour, with the solar farm accounting for the majority of the costs at \$9.44 per hour (91.6 %), attributed to the operational costs of 130 solar panels, each costing approximately \$0.07 per hour. The compression chiller contributes a smaller portion, with a cost rate of \$0.865 per hour (8.4 %). This breakdown highlights the cost-intensive nature of the solar farm in this system and underscores the importance of optimizing solar panel efficiency and maintenance schedules to reduce overall costs while maintaining system performance.

#### 4.4. Optimized solar farm outputs

This section presents the results of the optimized multi-generation solar farm, focusing on its capacity to generate heating, cooling, and electricity efficiently. These results demonstrate the system's ability to

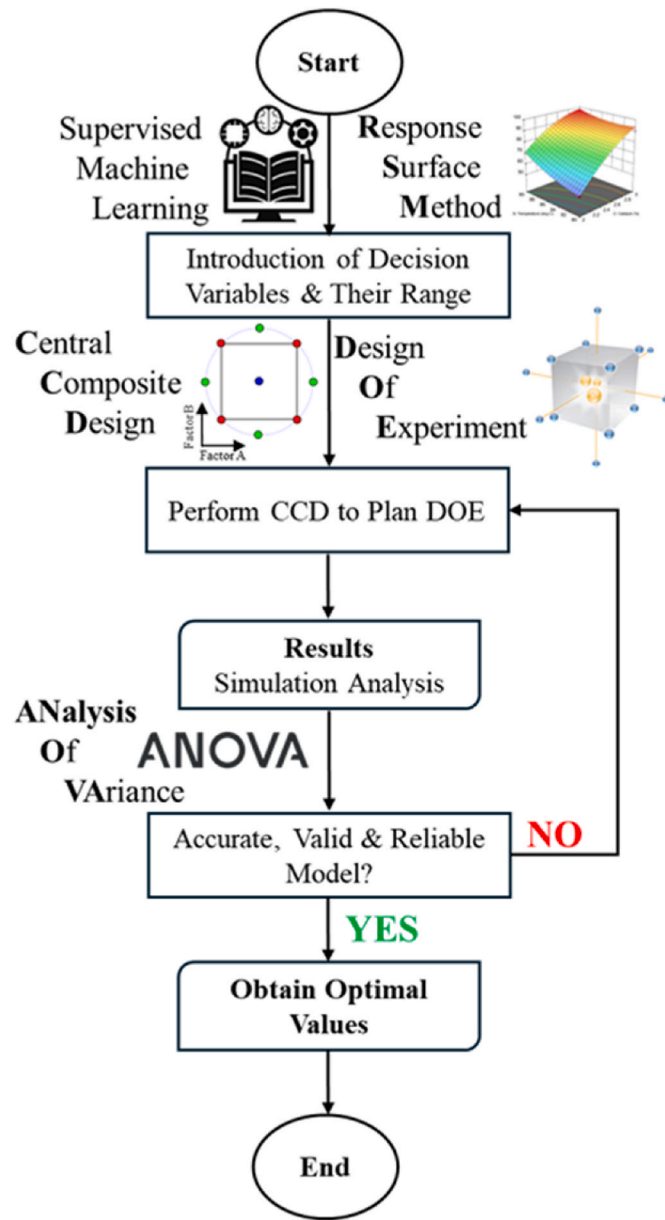


Fig. 11. Flowchart of the RSM process for optimizing solar farm.

**Table 4**  
Input data for the thermodynamic analysis of the solar farm.

| Parameter              | Unit                          | Amount |
|------------------------|-------------------------------|--------|
| $T_0$                  | $^{\circ}\text{C}$            | 25     |
| $P_0$                  | kPa                           | 101.3  |
| $n$                    | –                             | 90     |
| $T_{\text{sun}}$       | $^{\circ}\text{C}$            | 6000   |
| $\dot{m}_{\text{air}}$ | kg/s                          | 1.9    |
| $U_l$                  | $\text{W}/\text{m}^2\text{K}$ | 4.7    |
| $L$                    | m                             | 2.5    |
| $B$                    | m                             | 0.8    |
| $A$                    | m                             | 2      |

adapt to weather variations and optimize energy output to meet demand. Fig. 16 illustrates the hourly variations in cooling, heating, and net power generation from the optimized solar farm, utilizing a compression chiller, and responding dynamically to weather fluctuations across different seasons and times of the year. The integration of the compression chiller, powered by electricity generated from the solar

**Table 5**  
Optimization variables and ranges for improving solar farm performance.

| Input Parameter | Unit         | Lower bound | Upper bound |
|-----------------|--------------|-------------|-------------|
| PV Panel Number | –            | 90          | 140         |
| PV Panel Width  | $\text{m}^2$ | 1           | 3           |
| PV Panel Length | $\text{m}^2$ | 3           | 6           |

**Table 6**  
Optimal solution for decision parameters and objective functions.

| Optimal Input Parameters (PV Panel) |               |        |
|-------------------------------------|---------------|--------|
| Input Parameter                     | Unit          | Amount |
| Number                              | –             | 130    |
| Width                               | $\text{m}^2$  | 1.423  |
| Length                              | $\text{m}^2$  | 3.634  |
| Optimal Performance Metrics         |               |        |
| Metric                              | Unit          | Amount |
| Exergy Efficiency                   | %             | 25.699 |
| Cost Rate                           | $\$/\text{h}$ | 10.15  |
| Desirability                        | –             | 0.801  |

farm, facilitates efficient and simultaneous production of cooling and heating, minimizing energy waste and enhancing system utility. The hourly cooling energy varies significantly throughout the year, peaking at up to 8000 kWh during warmer months, aligning with seasonal temperature demands and showcasing the system's adaptability to climatic variations. Similarly, the heating energy fluctuates hourly, ranging from 0 to 10,000 kWh, with higher outputs during cooler periods, particularly in winter, following weather-dependent solar availability to ensure energy efficiency and reliability.

Fig. 16 also indicates that the solar farm's electricity generation ranges from 0 to 14,000 kWh, with seasonal and daily variations evident. Power outputs are higher during sunnier months and lower during periods of reduced solar irradiance, reflecting the impact of environmental conditions on solar energy generation. These results highlight the solar farm's ability to effectively respond to hourly, daily, and seasonal variations, meeting energy demands for cooling, heating, and electricity while generating surplus energy for storage or grid supply. This performance underscores the sustainability and efficiency of the optimized system in dynamic real-world conditions.

#### 4.5. Comparison of solar farm energy generation and case study demand

This section provides a comparative analysis of energy consumption and generation for cooling, heating, and electricity by the optimized solar farm, demonstrating its capability to fully meet the energy demands of the simulated Engineering and Technology Faculty at IAUD in Dezful while generating surplus energy for storage or other uses.

Fig. 17 compares the hourly and monthly variations in cooling energy produced by the solar farm versus the cooling energy consumed by the case study. This representation highlights the dynamic response of cooling production to fluctuating daily, monthly, and seasonal climatic conditions, showing how production and consumption patterns evolve over the year. The figure demonstrates that the solar farm produces a total of 12,869,716.61 kWh of cooling energy annually, while the faculty requires 7,517,506.279 kWh, resulting in a significant surplus of 5,352,210.329 kWh. On a daily and seasonal basis, the hourly cooling production peaks during warmer months, with surplus energy consistently available during midday hours when solar radiation is at its highest. Monthly data further confirm that cooling production exceeds consumption during all months, particularly from May to September, aligning with increased cooling demands during summer in hot climates. This surplus energy, especially pronounced during summer, can be stored for future use, addressing cooling demands during nighttime or

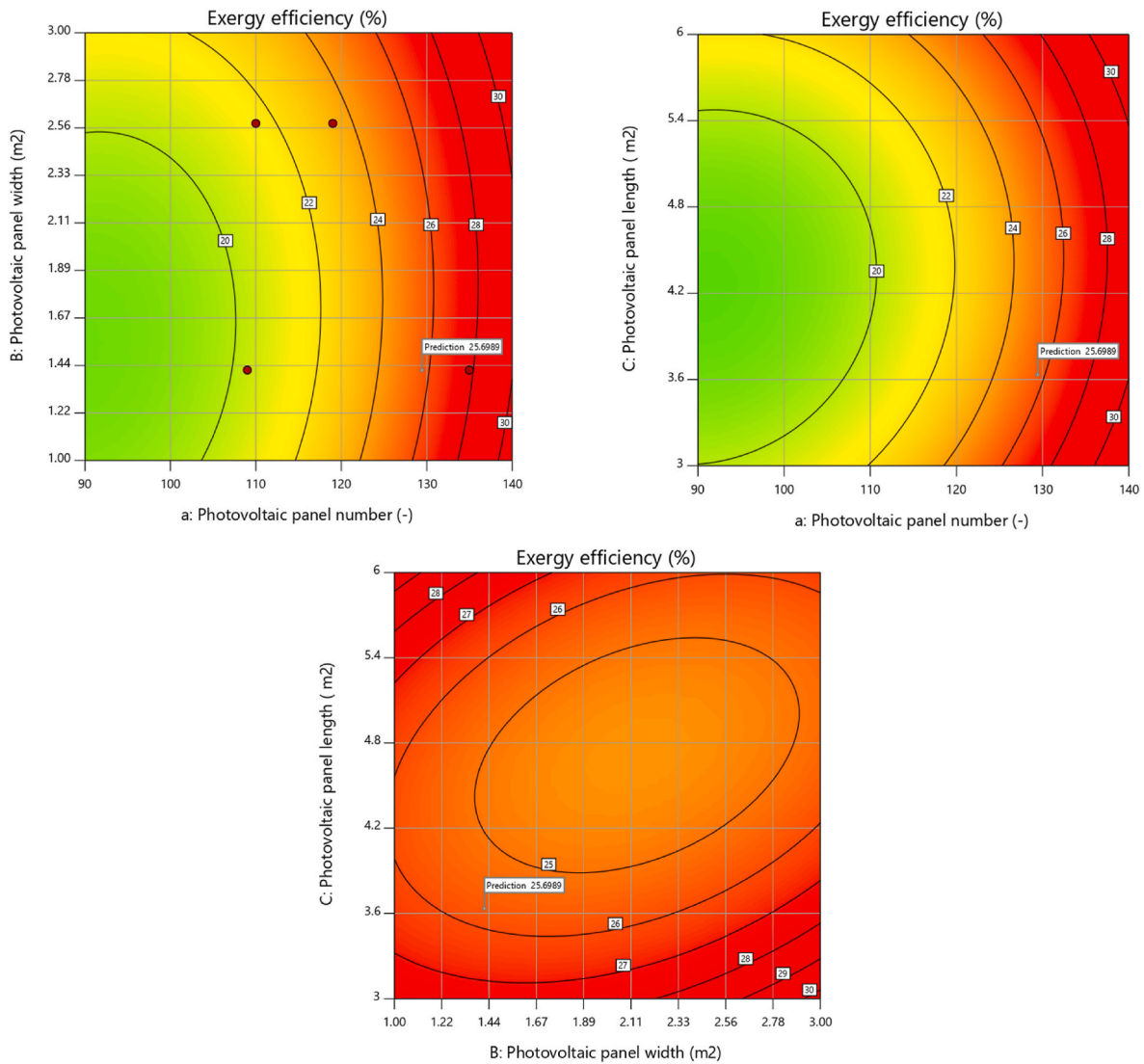


Fig. 12. Impact of three input variables: Number, width, and length of PV panel on exergy efficiency.

less sunny periods, thereby enhancing system efficiency and utility.

Fig. 18 shows the hourly and monthly variations in generated heating energy versus the usage by the case study. This figure highlights the daily, monthly, and seasonal variations in heating production, indicating changes in production and usage patterns over the year. The solar farm produces a total of 17,990,632.41 kWh of heating energy annually, while the faculty requires only 6571.73 kWh, resulting in a surplus of 17,984,060.67 kWh. This surplus is substantially higher than the cooling energy surplus identified in Fig. 17, where the solar farm produced an excess of 5,352,210.329 kWh, representing an increase of approximately 236 %. On a daily and seasonal basis, the hourly heating production peaks during cooler months, aligning with periods of lower ambient temperatures and increased heating demand, while surplus energy remains consistently available even during periods of lower consumption. Monthly data confirm that heating production far exceeds consumption across all months, particularly from April to September, when heating needs are minimal.

The substantial surplus heating energy is utilized in an absorption cooling cycle to meet the cooling demands of the case study, directly reducing the load on electric cooling systems and improving energy efficiency. This setup not only supports the institution's cooling needs but also ensures that any surplus energy can be stored for future use or supplied to neighboring facilities, depending on the availability of

suitable distribution infrastructure. This dual-purpose use of heating energy for cooling during warmer months highlights the system's flexibility and maximizes the utility of the heat generated. It aligns with the research objective of developing sustainable and efficient energy systems capable of meeting diverse energy demands in dynamic real-world conditions.

Fig. 19 compares the hourly and monthly variations in electricity produced by the solar farm versus the electricity consumed by the case study. This representation highlights the solar farm's ability to dynamically respond to daily, monthly, and seasonal climatic variations, showcasing the evolution of production and consumption patterns throughout the year. The figure demonstrates that the solar farm generates a total of 22,811,138.02 kWh of electricity annually, while the faculty requires 18,237,329.59 kWh, resulting in a surplus of 4,573,808.425 kWh, which is 25 % above consumption. In comparison, the heating energy surplus is 17,984,060.67 kWh or approximately 273 % above heating consumption, and the cooling energy surplus is 5,352,210.329 kWh, or about 71 % above cooling consumption. The comparison between cooling, heating, and power surplus indicates that electricity surplus is the smallest relative to its demand but still contributes significantly to operational cost savings and grid supply.

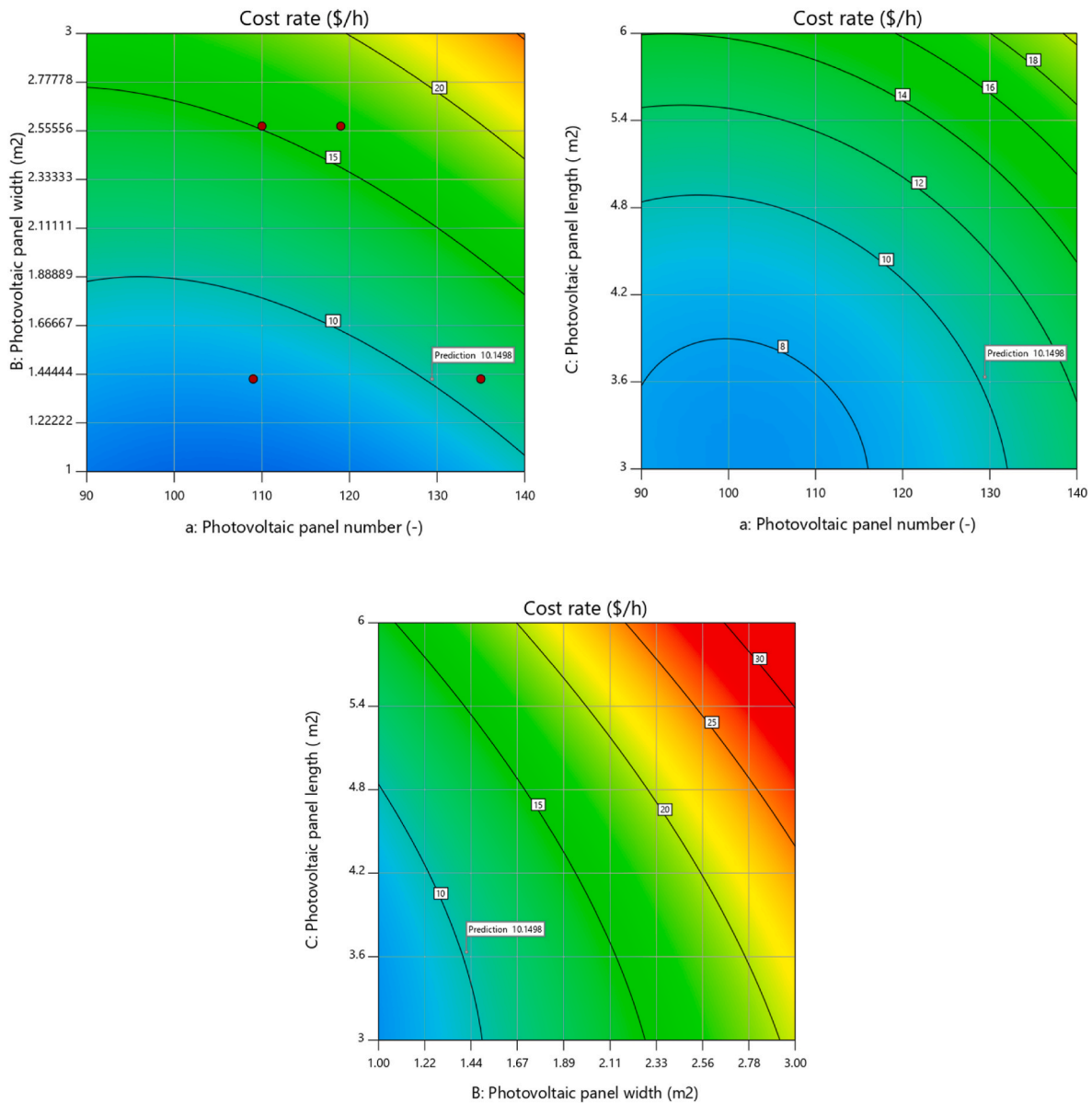


Fig. 13. Impact of three input variables: Number, width, and length of PV panel on cost rate.

#### 4.6. Surplus energy storage and utilization

The investigation into the solar farm's ability to supply energy for the case study demonstrates its strong capacity to efficiently meet energy demands while also generating significant surplus cooling, heating, and power annually. This surplus energy can be stored for future use, supplied to nearby facilities, or exported to the national grid, thereby enhancing the system's economic viability and contributing to sustainable energy practices.

Fig. 20 presents a detailed monthly analysis of the surplus cooling energy stored in a year, calculated as the difference between the cooling energy generated and consumed by the case study. The results indicate that the stored cooling energy notably fluctuates with seasonal variations. The highest surplus cooling energy is observed in March at 785,175.06 kWh, approximately 400 % higher than the lowest value of 156,998.94 kWh recorded in August. This difference highlights the stark contrast between the cooler and warmer months, with surplus cooling energy during cooler months such as January to April averaging 679,249 kWh, which is more than 260 % greater than the monthly average for the warmer period from July to September (approximately

186,809 kWh). This seasonal trend highlights the capability of generating the highest surplus cooling energy during periods of lower demand, such as in late winter and early spring when cooling requirements are minimal and solar radiation is still strong. The stored cooling energy from these months can be effectively utilized during periods of higher demand, such as the summer months, or repurposed for alternative applications, thereby enhancing the overall efficiency and sustainability of the system.

Fig. 21 illustrates the monthly assessment of heating energy stored in a year, calculated as the difference between the produced heating energy, powered by its own compression chiller unit, and the heating usage. The results demonstrate that the solar farm consistently generates surplus heating energy, with the highest surplus observed in July at 2,144,206 kWh and the lowest in December at 810,322 kWh, representing a 165 % increase. The mean surplus heating energy during warmer months (May to August) averages 2,000,263 kWh per month, aligning with high production due to favorable solar conditions and minimal heating demand. In contrast, during cooler months (November to January), the average surplus drops to approximately a third of warmer months, 871,079 kWh, aligning with increased heating needs.

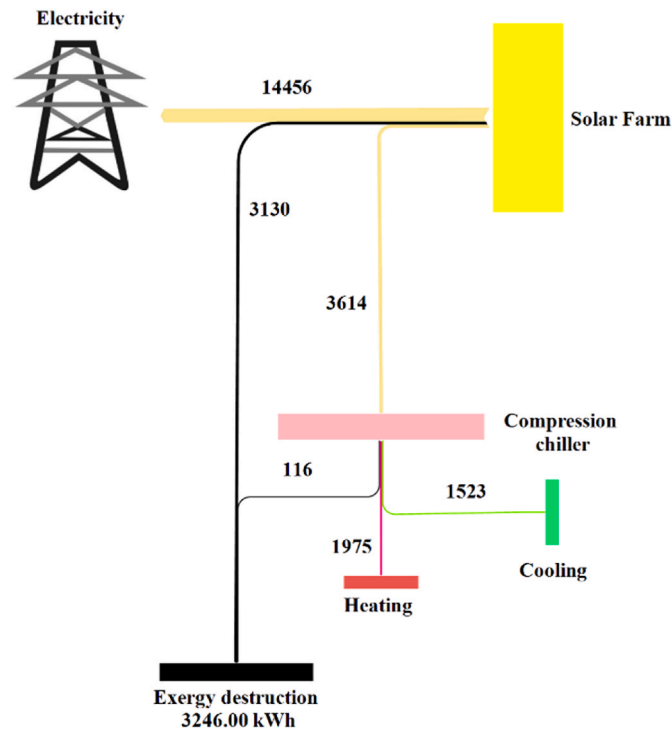


Fig. 14. Total exergy destruction rate and contributions from individual components.

Unlike cooling energy, where the highest surpluses occur in cooler months with minimal demand, heating surpluses are more evenly distributed throughout the year, with peaks in months where solar production is highest. These seasonal variations highlight the solar farm's ability to adapt to fluctuating climatic conditions while ensuring sufficient energy is stored during periods of high output. This stored energy can be repurposed for secondary applications, such as absorption cooling or supplying neighboring facilities, enhancing the overall efficiency, utility, and sustainability of the system.

Fig. 22 presents the monthly calculations of surplus electricity generated by the solar farm, categorized as stored electricity annually. This surplus is calculated as the difference between the total electricity generated by the solar farm's 130 PV panels and the electricity consumed by the case study. The highest surplus is observed in March at 829,877 kWh, while the lowest occurs in October at just 1136 kWh, reflecting a sharp seasonal variation driven by solar irradiance. Surpluses are significant during the spring and early summer months, including April (735,537 kWh) and June (767,479 kWh), whereas late autumn and winter months experience minimal surpluses due to lower solar irradiance and shorter daylight. This trend highlights the solar farm's capacity to generate and store substantial electricity during high-production months, ensuring efficient energy use and providing the potential for grid export to enhance economic returns and support sustainable energy practices.

The optimal configuration of 130 PV panels enables the solar farm to consistently generate a significant surplus of cooling, heating, and electricity, reflecting its adaptability to varying energy demands and seasonal conditions. This surplus capacity not only ensures the energy self-sufficiency of the case study but also creates opportunities for additional revenue generation through grid exports, particularly during months of high production. Furthermore, surplus cooling and heating energy can be effectively repurposed for secondary applications, such as powering absorption chillers or supplying nearby facilities, thereby reducing dependency on conventional energy sources. By leveraging advanced storage solutions and optimizing energy distribution, the system maximizes its economic feasibility while supporting local energy

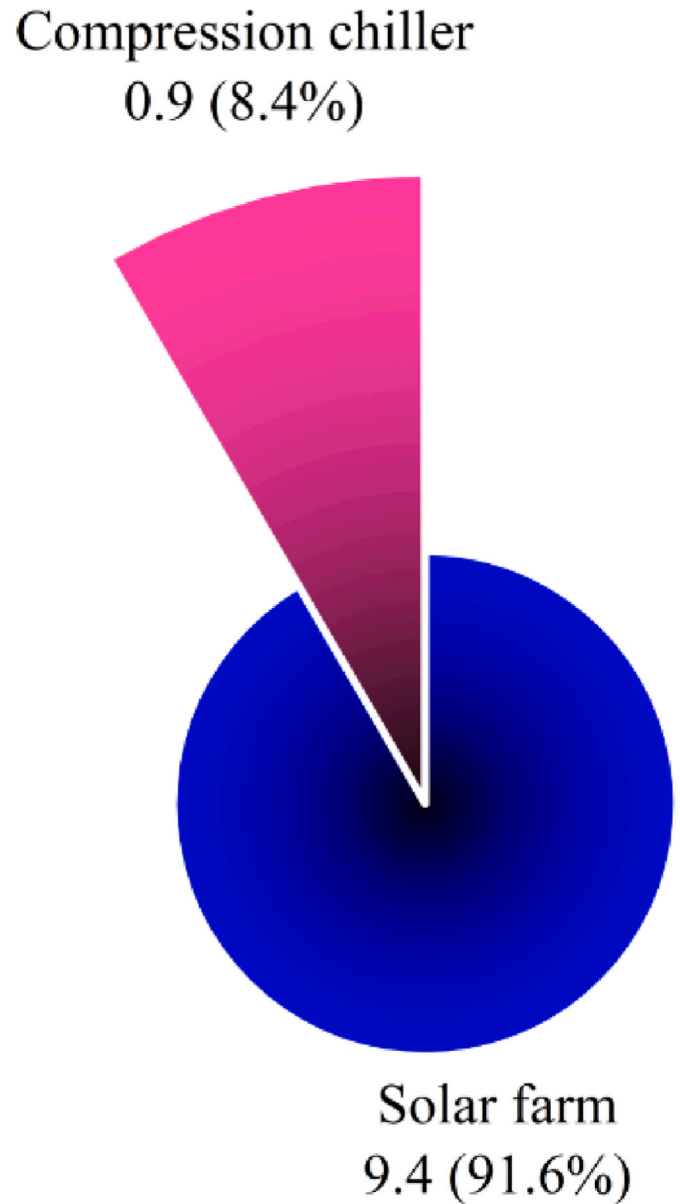


Fig. 15. Total cost rate of the system and its primary components.

needs and aligning with sustainable energy management practices. This integration of surplus energy utilization demonstrates a holistic approach to resource efficiency, contributing to broader goals of environmental sustainability and energy resilience.

#### 4.7. Environmental benefits of solar farm

Fig. 23 highlights the ecological benefits of the solar farm supplying power to the case study. The integration of machine learning optimizes energy generation, helping to meet environmental goals by reducing fossil fuel dependency and lowering carbon emissions.

The solar farm produces a net output of 22,745.14 MWh, effectively replacing energy that would otherwise be generated by conventional power plants emitting approximately 0.204 tons of CO<sub>2</sub> per MWh. This reduction translates to a total mitigation of 4640.008 tons of CO<sub>2</sub> annually, equivalent to an ecological cost saving of \$111,360, based on a carbon cost of \$24 per ton of CO<sub>2</sub>. This reduction is environmentally significant, comparable to the positive impact of adding 22 ha of green spaces. By implementing the solar farm, environmental costs are minimized throughout the year, helping to mitigate pollution emissions

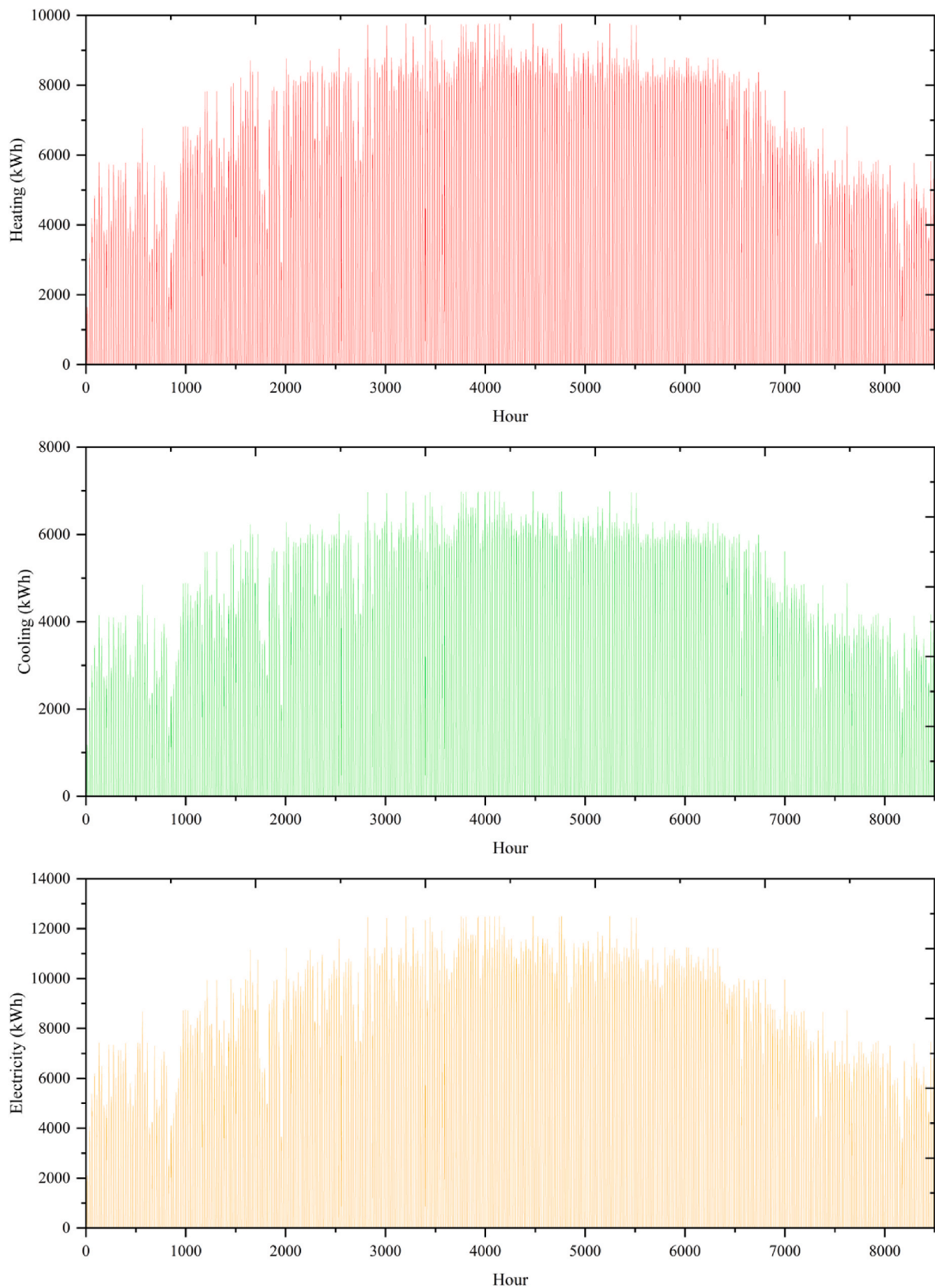


**Fig. 16.** Hourly variations in cooling, heating, and electricity generation of the optimized solar farm.

while optimizing energy consumption for the faculty. The ability to generate surplus energy also highlights its potential for economic savings and revenue generation, particularly through grid exports and exploring options for utilizing surplus heating and cooling energy through partnerships or storage. This dual focus on reducing greenhouse

gas emissions and enhancing resource efficiency positions the solar farm as a sustainable energy solution, advancing the transition to eco-friendly practices in large-scale facilities, such as university campuses (Alirahmi et al., 2021; Kroeger et al., 2014).

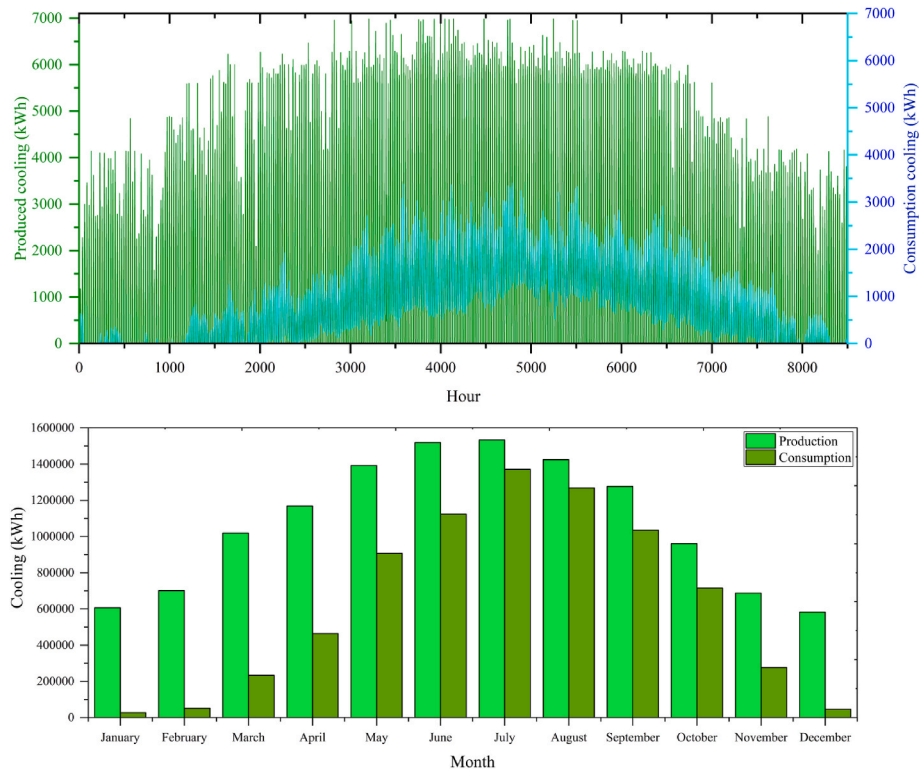


Fig. 17. Comparison of the generated cooling energy with cooling energy usage.

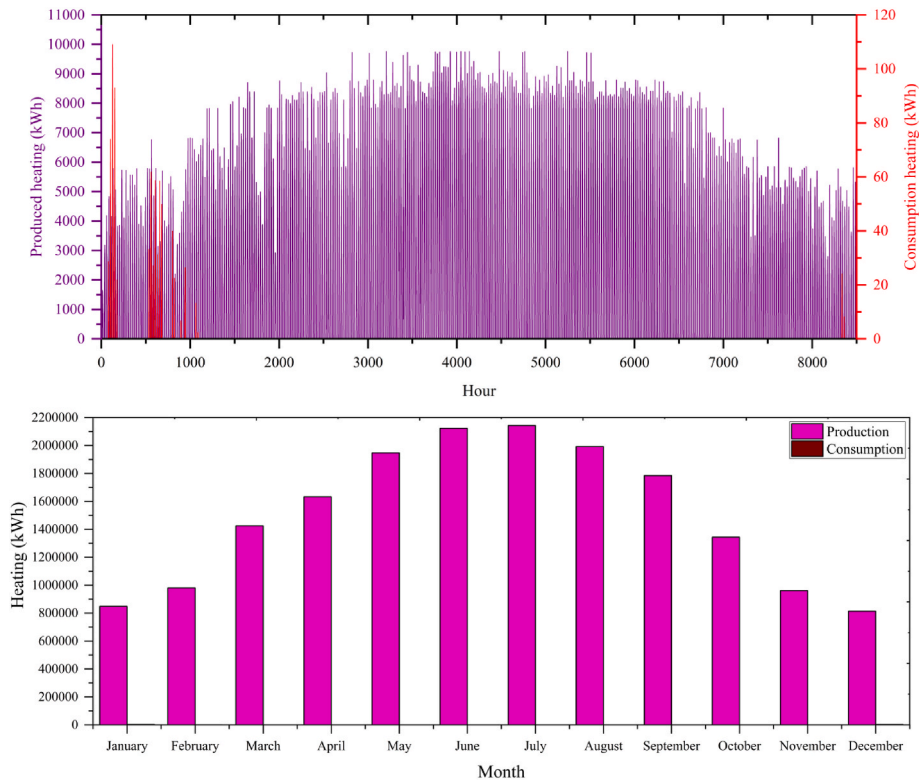


Fig. 18. Comparison of the generated heating energy heating with heating consumption.

4.8. Scalability and modularity design

The proposed solar farm’s design emphasizes scalability and modularity, ensuring adaptability to varying energy demands and site

conditions, even in severe climates like Dezful, where extreme temperatures and fluctuating solar irradiance pose significant challenges for energy systems. By utilizing a modular configuration of 130 PV panels integrated with machine learning-driven optimization using RSM, the

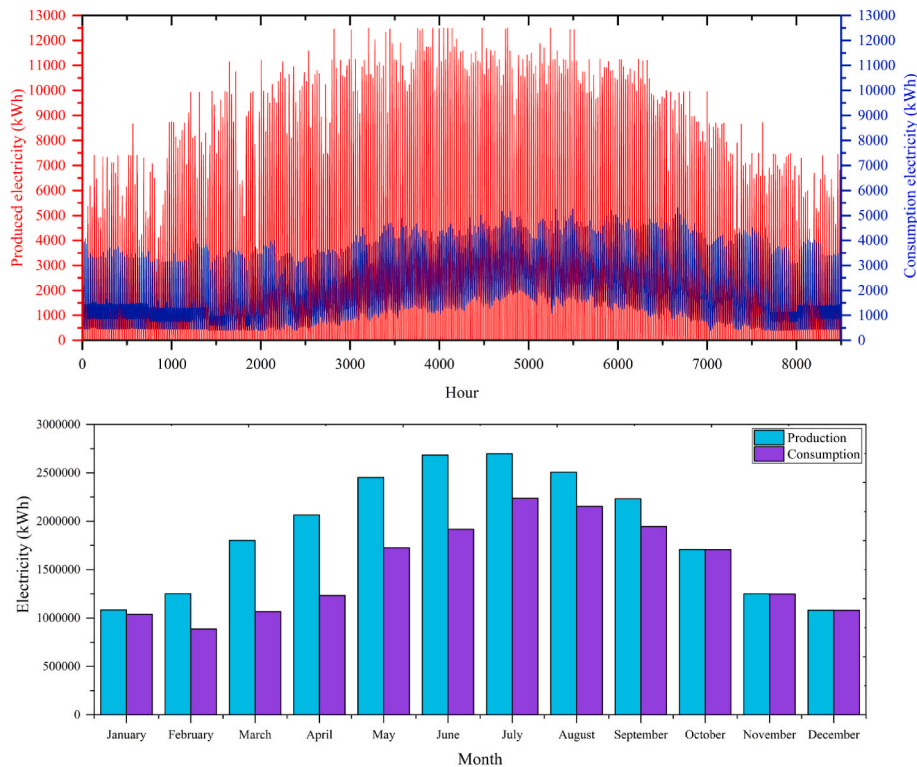


Fig. 19. Comparison of produced electricity and consumption.

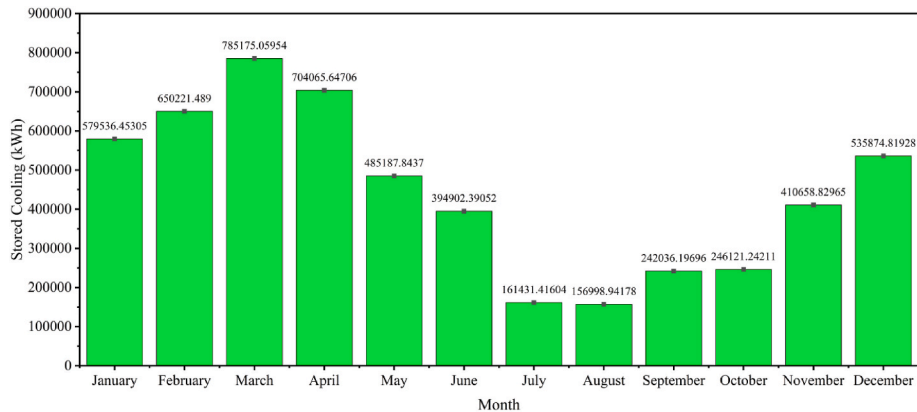


Fig. 20. Monthly surplus cooling energy stored by the solar farm.

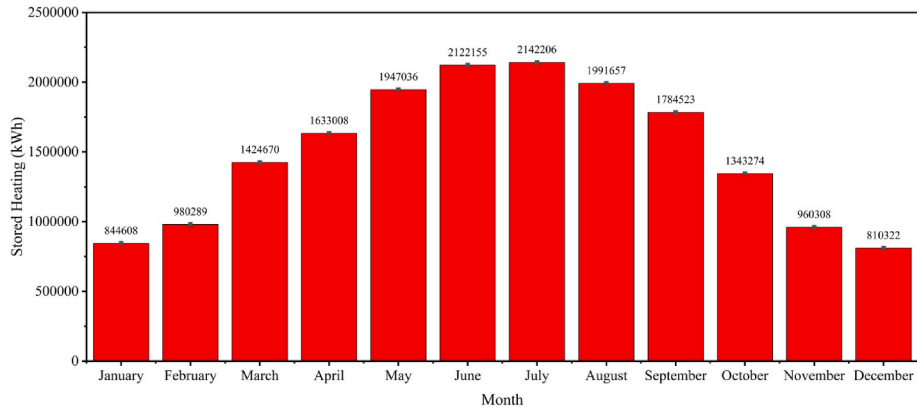


Fig. 21. Monthly surplus heating energy stored by the solar farm.

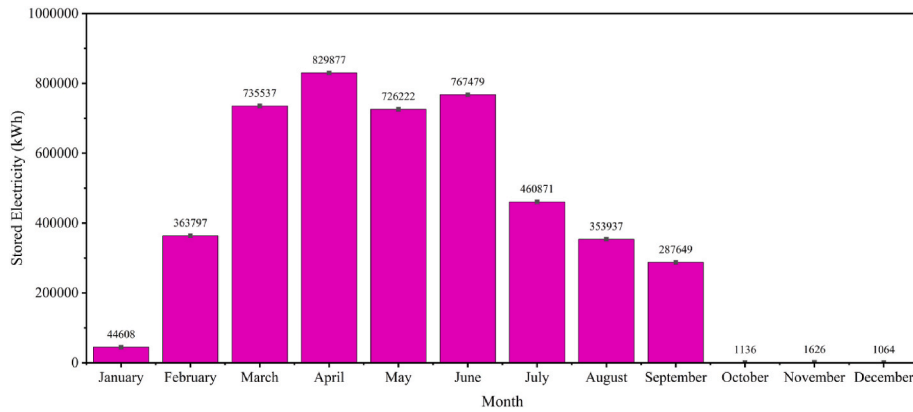


Fig. 22. Monthly surplus electricity generated and stored by the solar farm.

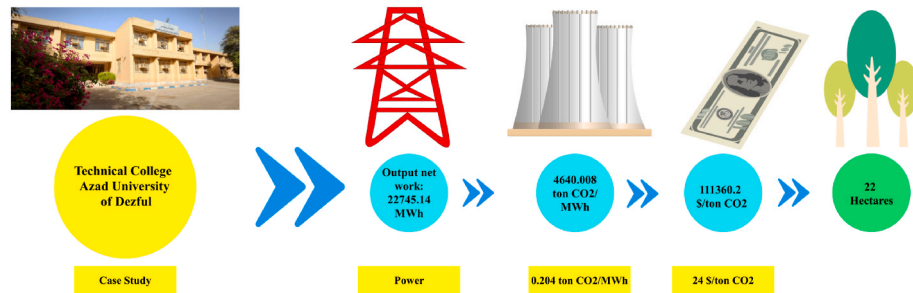


Fig. 23. Environmental benefits of the solar farm.

design can be expanded or reconfigured to meet the needs of larger facilities or scaled down for smaller applications. RSM, framed as a lightweight supervised learning technique, facilitates the optimization of modular configurations by leveraging labeled input-output data, ensuring efficient adaptation to changing energy demands and site-specific conditions. This flexibility allows the system to accommodate future energy requirements, such as the integration of additional facilities or community-wide energy solutions. The modular nature of the design also simplifies maintenance and upgrades, reducing operational downtime and costs, while enabling gradual system expansion in response to budget constraints or increased energy demand.

This scalable and modular approach addresses the research objective of creating a sustainable, efficient energy system capable of adapting to real-world challenges, such as seasonal energy variability, growing energy demands, and the complex needs of multifunctional facilities, such as university buildings. By leveraging modularity, the solar farm enhances resource efficiency and its applicability to diverse geographic locations and building types. The system's ability to integrate with existing infrastructure, such as supplying surplus energy to neighboring facilities or exporting electricity to the grid, further highlights its practicality and economic viability. This design philosophy bridges the gap identified in the research by demonstrating how renewable energy systems can provide tailored, flexible solutions for large-scale, multifunctional applications, contributing to the transition toward more sustainable and resilient energy systems.

#### 4.9. Comparison with previous system

This section evaluates the designed and optimized solar farm, comparing its performance, cost-effectiveness, and environmental benefits with previously introduced systems in the literature. Table 7 presents a detailed comparison of the current system with earlier models by outlining system descriptions, utilized optimization methods, and performance metrics. Key parameters such as cost rate, exergy efficiency,

and CO<sub>2</sub> reduction are compared with the previous systems.

Table 7 demonstrates that the proposed optimized multi-generation system exhibits competitive performance compared to prior studies. With an exergy efficiency of 25.69 % and a cost rate of \$10.15/hour, the system effectively balances technical and economic objectives. By leveraging RSM as a lightweight supervised machine learning technique, this study efficiently models and optimizes key input-output relationships, ensuring a balance between performance and cost. Although its exergy efficiency is lower than some advanced systems, such as the solar gas turbine-based multi-generation system with an exergy efficiency of 60.05 % (Cao et al., 2020) and the intelligent building-integrated system with an efficiency of 44.9 % (Saadmohammadi and Sajadi, 2024), it outperforms most in cost-effectiveness. The cost rate is significantly lower than comparable systems, such as the hybrid solar-biomass multi-generation system with a total cost rate of \$324.60/hour (Korpeh et al., 2024) and the solar tower-based gas turbine-driven plant with a cost rate of \$184.8/hour (Colakoglu and Durmayaz, 2022b). This highlights the system's economic feasibility and scalability for large-scale academic institutions, aligning with the research's aim to provide sustainable energy solutions for high-demand environments.

In terms of environmental benefits, the proposed system achieves a substantial CO<sub>2</sub> reduction of 7395 tons per year, rivaling larger systems such as the hybrid solar-biomass configuration, which achieves approximately 8305 tons/year (Korpeh et al., 2024), and surpassing the solar tower-based plant, which achieves around 4501.6 tons/year (Colakoglu and Durmayaz, 2022a). While the optimized multi-generation system does not reach the exceptional exergy efficiency of certain models, its integration of machine learning-driven optimization using RSM sets it apart as a computationally efficient and interpretable solution, ideal for balancing multi-objective trade-offs in cost, efficiency, and environmental impact. This balance of cost, efficiency, and environmental impact positions the proposed system as a viable option for sustainable energy management in large-scale, multifunctional facilities such as university campuses.

**Table 7**  
Comparison of performance metrics, cost, and environmental impact.

| Ref                             | System Description   | Optimization Method  | Cost Rate (\$/hour)  | Exergy Efficiency (%) | CO <sub>2</sub> Reduction                                |
|---------------------------------|--|--|----------------------|-----------------------|--|
| Current System                  | Multi-generation solar farm for university campus integrating PV panels and compression chiller to produce cooling, heating, and electricity.  | Multi-objective optimization using RSM, BEopt, and EES   | 10.15                | 25.69                 | 7395 (tons/year)   |
| Saadmohammadi and Sajadi (2024) | Intelligent building-integrated solar cogeneration system with PV panels, evacuated tube collectors, absorption chiller, and desalination unit.  | Machine learning and genetic algorithm   | N.A.                 | 44.9                  | 0.158 tons/MWh (3.29 tons/year, if works 24 h, 365 days) |
| Mouaky and Rachek (2024)        | Hybrid solar-biomass multi-generation system integrating an Organic Rankine Cycle (ORC) for electricity, hot water, and membrane distillation for RO brine minimization.                           | NSGA-II algorithm and TOPSIS decision-making tool  | 93.01 (~87.68 €/h)   | 5.39                  | N.A.   |
| Korpeh et al. (2024)            | Hybrid solar-biomass multi-generation system to supply heating, cooling, electricity, fresh water, and hydrogen, with solar and biomass as energy sources.   | Multi-objective optimization (Two-category optimization considering economic and environmental objectives) | 324.60               | 31.75                 | 3.55 tons/MWh (8305 tons/year, if works 24 h, 365 days)  |
| Yadav et al. (2023)             | Solar-concentrated photovoltaic-thermal collector integrated poly-generation system for power, cooling, and freshwater supply using eco-friendly refrigerants.                                     | Energy, exergy, economic, and environmental analysis across various operating conditions.                  | 0.70                 | 4.15                  | 301.7 tons/year  |
| Esmaeilion et al. (2022)        | Multi-generation hybrid solar and wind, incorporating solar cycles and hydrogen generation, to produce cooling, heating, electricity, freshwater, and hydrogen.                                    | Multi-objective particle swarm optimization  | 61.2 \$/GJ (~220.32) | 41.07                 | 2965.45 tons/year  |
| Colakoglu and Durmayaz (2022a)  | Solar tower-based multi-generation system integrating Brayton, organic Rankine, and Goswami cycles for power, heating, cooling, freshwater, and hydrogen production.                               | Multi-objective optimization considering thermodynamic and economic objectives                             | 92.3                 | 37.99                 | 513.8 kg CO <sub>2</sub> /h (~4501.6 tons/year)          |
| Colakoglu and Durmayaz (2022b)  | Solar tower-based gas turbine-driven multi-generation plant integrating intercooling-regenerative-reheat gas turbine, organic Rankine cycles, and various utilities for multi-generation products. | Multi-objective optimization including energy, exergy, economic, and environmental indicators              | 184.8                | 40.7                  | 948.7 kg CO <sub>2</sub> /h (~8312 tons/year)            |
| Cao et al. (2020)               | Solar gas turbine-based multi-generation system with organic Rankine cycle, desalination unit, LNG cold energy recovery, and absorption chiller.   | MOSPO algorithm, compared with NSGA-II, MOPSO, PESA-II, SPEA-II  | 36.75                | 60.05                 | 485 tons/year  |

**5. Limitations and future work**

This study demonstrates the feasibility and optimization of a solar-powered multi-generation system for university campuses; however, limitations should be acknowledged. First, the analysis assumes steady-state operating conditions, neglecting dynamic variations in energy demand and environmental conditions throughout the year. While this assumption simplifies modeling, it may overlook transient effects, such as fluctuating solar irradiance and sudden shifts in cooling or heating demands. Second, the study focuses solely on solar energy as the primary renewable source, limiting the system’s adaptability to complementary energy sources like wind or biomass, which could enhance resilience during periods of low solar output. Third, the economic analysis does not account for external factors, such as maintenance costs due to PV panel degradation or potential disruptions in supply chains for replacement components. Fourth, the model assumes negligible pressure drops and energy losses in pipelines, which could result in slight inaccuracies in the thermodynamic calculations for larger-scale applications. Lastly, RSM has limitations, including reduced effectiveness for systems with a high number of variables or highly nonlinear interactions, where algorithms like neural networks may perform better, and its focus on steady-state conditions, which may require additional tools for transient modeling.

Future research could build upon the findings by addressing the outlined limitations to enhance the robustness and applicability of the proposed system. Incorporating dynamic modeling tools to capture transient variations in energy demand and supply, such as those caused by weather fluctuations or peak usage periods, would provide a more accurate assessment of system performance. Integrating advanced machine learning techniques, such as real-time predictive algorithms or

reinforcement learning, alongside RSM, could enable dynamic optimization and improve adaptability in fluctuating conditions. Exploring hybrid renewable energy systems by integrating wind, biomass, or geothermal sources could improve system resilience and year-round energy reliability. Real-time energy management systems using predictive algorithms and IoT sensors could also be developed to dynamically optimize system operations, further enhancing cost-effectiveness and efficiency. To extend the practical application, future studies could investigate the scalability of the proposed design across varying geographic and institutional contexts, particularly for regions with less solar availability or higher energy demands. Finally, long-term economic assessments, including lifecycle costs and sustainability metrics, would offer a comprehensive evaluation of the system’s economic and environmental benefits.

**6. Conclusion**

This study aimed to address the challenges of rising energy demand, operational costs, and environmental impact in university buildings by designing and optimizing a multi-generation solar farm using a Machine Learning-driven Multi-Objective Optimization framework. By integrating BEopt and Engineering Equation Solver software with Response Surface Methodology, framed as a lightweight supervised machine learning technique, the system was optimized to maximize exergy efficiency and minimize costs while addressing the specific energy demands of a case study university building in Dezful, Iran. The proposed system achieved notable results, including an exergy efficiency of 25.69 % and an operational cost of \$10.15 per hour. It also generated 22.8 GWh of electricity, 17.9 GWh of heating, and 12.9 GWh of cooling annually, surpassing the building’s energy demands and contributing to a CO<sub>2</sub>

emissions reduction of approximately 7395 metric tons per year.

From these results, the study's key findings are as follows.

- The use of RSM as part of a supervised machine learning framework facilitated efficient modeling of input-output relationships, enabling optimization across multiple objectives.
- The system's ability to consistently generate surplus electricity (4.56 GWh annually) demonstrates effective energy utilization and economic viability by providing potential revenue streams through energy export or additional applications.
- Achieving an exergy efficiency of 25.69 % highlights the optimized balance of energy use across multiple outputs, validating the research objective to enhance the quality of energy utilization in solar-powered systems for large-scale applications.
- The operational cost of \$10.15 per hour reflects a substantial reduction in energy expenses compared to fossil-fuel-based systems, addressing the study's aim of ensuring cost-efficiency for high-demand environments.
- The CO<sub>2</sub> emissions reduction (7395 metric tons annually) underscores the environmental benefits of transitioning to a renewable energy-based system, fulfilling global sustainability goals and demonstrating alignment with climate change mitigation strategies.
- The modular and scalable design of the system ensures its adaptability and applicability across diverse contexts, supporting the research objective to create a replicable framework for sustainable energy management.

These findings contribute to the broader field of sustainable energy systems by demonstrating how solar-powered multi-generation designs can exceed energy demands, reduce costs, and significantly mitigate environmental impacts. By framing RSM as part of a machine learning-driven framework, this study highlights the role of interpretable and computationally efficient optimization methods in advancing renewable energy solutions. Future work should focus on integrating dynamic

modeling tools for real-time optimization, exploring hybrid renewable sources to improve resilience, and validating the system's scalability in varying geographic and institutional contexts. Such efforts could further advance the practicality and sustainability of multi-generation energy systems for multifunctional buildings worldwide.

#### CRediT authorship contribution statement

**Ehsanolah Assareh:** Writing – review & editing, Writing – original draft, Visualization, Validation, Software, Methodology, Investigation, Formal analysis, Data curation, Conceptualization. **Nima Izadyar:** Writing – review & editing, Writing – original draft, Validation, Supervision, Project administration, Investigation, Formal analysis, Resources, Visualization. **Elmira Jamei:** Writing – review & editing, Resources, Methodology. **Mohammad amin Monzavian:** Writing – review & editing, Visualization, Data curation. **Saurabh Agarwal:** Writing – review & editing, Conceptualization, Formal analysis, Validation. **Wooguil Pak:** Supervision, Project administration, Resources, Writing – review & editing.

#### Declaration of Generative AI

During the preparation of this work, the authors used an OpenAI tool to enhance language and readability. After using the tool, the authors reviewed and edited the content as needed. They take full responsibility for the final content of the publication. The authors highlight that AI's role was to assist in refining the text and language, and not to replace any critical tasks of the authors.

#### Declaration of competing interest

The authors declare that they have no known competing financial interests or personal relationships that could have appeared to influence the work reported in this paper.

## Appendix A. Thermodynamic Relationships for Solar Farm Analysis

To conduct the thermodynamic analysis of the solar farm, fundamental equations are applied in the discussion. Table A.1 presents the key relationships used in this analysis, providing the essential formulas for evaluating the solar farm's performance.

Table A.1 Thermodynamic analysis

| Fundamental Concepts        | Relationship   |
|-----------------------------|--|
| Law of conservation of mass | $\sum_k \dot{m}_i - \sum_k \dot{m}_e = \frac{dm_{cv}}{dt}$   |
| Conservation of Energy      | $\dot{Q} - \dot{W} + \sum_i \dot{m}_i \left( h_i + \frac{v_i^2}{2} + gZ_i \right) - \sum_e \dot{m}_e \left( h_e + \frac{v_e^2}{2} + gZ_e \right) = \frac{dE_{cv}}{dt}$ |
| Exergy Balance              | $\dot{E}x_Q + \sum_i \dot{m}_i (ex_i) = \sum_e \dot{m}_e (ex_e) + \dot{E}x_W + \dot{E}x_D$   |
| Physical Exergy             | $\dot{E}x_{ph} = \sum_i \dot{m}_i ((h_i - h_0) - T_0(s_i - s_0))$  |
| Cost Rate                   | $\dot{Z} = \frac{Z \times CRF \times \varphi}{T}$  |
| Capital Recovery Factor     | $CRF = \frac{k(1+k)^n}{(1+k)^n - 1}$   |

## Appendix B. Results of 100 Optimal Points Based on Desirability Levels

Appendix B provides the results for 100 data points analyzed through RSM, where each data point represents a combination of input variables assessed to model exergy efficiency and cost behavior. This dataset supports the creation of response surfaces, which are essential for determining optimal values within the broader tested range. Table B.1 presents the outcomes of 100 optimal points evaluated according to their desirability levels.

Table B.1 Outcomes of 100 Optimal points

| Number | PV panel number (–) | PV panel width (m <sup>2</sup> ) | PV panel length (m <sup>2</sup> ) | Exergy efficiency (%) | Cost rate (\$/h) | Desirability |
|--------|---------------------|----------------------------------|-----------------------------------|-----------------------|------------------|--------------|
| 1      | 130                 | 1.423                            | 3.634                             | 25.699                | 10.15            | 0.801        |
| 2      | 129.237             | 1.423                            | 3.634                             | 25.629                | 10.117           | 0.8          |
| 3      | 129.433             | 1.423                            | 3.642                             | 25.684                | 10.161           | 0.8          |
| 4      | 129.433             | 1.423                            | 3.648                             | 25.671                | 10.17            | 0.8          |
| 5      | 129.433             | 1.429                            | 3.634                             | 25.693                | 10.187           | 0.8          |
| 6      | 129.111             | 1.425                            | 3.634                             | 25.582                | 10.112           | 0.799        |
| 7      | 128.868             | 1.423                            | 3.634                             | 25.5                  | 10.056           | 0.799        |
| 8      | 129.434             | 1.432                            | 3.635                             | 25.688                | 10.21            | 0.799        |
| 9      | 129.434             | 1.423                            | 3.658                             | 25.653                | 10.184           | 0.799        |
| 10     | 129.434             | 1.428                            | 3.648                             | 25.666                | 10.202           | 0.799        |
| 11     | 128.729             | 1.423                            | 3.634                             | 25.451                | 10.033           | 0.799        |
| 12     | 129.433             | 1.423                            | 3.665                             | 25.64                 | 10.194           | 0.799        |
| 13     | 129.242             | 1.423                            | 3.664                             | 25.574                | 10.16            | 0.798        |
| 14     | 129.434             | 1.438                            | 3.634                             | 25.683                | 10.245           | 0.798        |
| 15     | 129.433             | 1.423                            | 3.679                             | 25.613                | 10.215           | 0.798        |
| 16     | 128.202             | 1.423                            | 3.634                             | 25.268                | 9.949            | 0.797        |
| 17     | 129.434             | 1.423                            | 3.688                             | 25.597                | 10.228           | 0.797        |
| 18     | 129.434             | 1.447                            | 3.634                             | 25.674                | 10.301           | 0.797        |
| 19     | 127.864             | 1.423                            | 3.634                             | 25.152                | 9.893            | 0.797        |
| 20     | 129.433             | 1.455                            | 3.634                             | 25.667                | 10.351           | 0.795        |
| 21     | 129.434             | 1.423                            | 3.718                             | 25.543                | 10.274           | 0.795        |
| 22     | 129.434             | 1.461                            | 3.634                             | 25.661                | 10.386           | 0.795        |
| 23     | 127.192             | 1.424                            | 3.634                             | 24.923                | 9.798            | 0.795        |
| 24     | 129.434             | 1.423                            | 3.74                              | 25.506                | 10.307           | 0.794        |
| 25     | 129.434             | 1.472                            | 3.634                             | 25.651                | 10.457           | 0.793        |
| 26     | 128.854             | 1.469                            | 3.634                             | 25.45                 | 10.339           | 0.792        |
| 27     | 129.433             | 1.48                             | 3.634                             | 25.644                | 10.505           | 0.792        |
| 28     | 126.652             | 1.437                            | 3.634                             | 24.731                | 9.794            | 0.791        |
| 29     | 125.429             | 1.423                            | 3.634                             | 24.348                | 9.523            | 0.79         |
| 30     | 129.434             | 1.423                            | 3.846                             | 25.339                | 10.483           | 0.787        |
| 31     | 129.433             | 1.423                            | 3.866                             | 25.311                | 10.517           | 0.786        |
| 32     | 129.39              | 1.521                            | 3.634                             | 25.595                | 10.76            | 0.785        |
| 33     | 129.433             | 1.534                            | 3.634                             | 25.601                | 10.851           | 0.783        |
| 34     | 129.434             | 1.423                            | 3.947                             | 25.207                | 10.665           | 0.781        |
| 35     | 121.432             | 1.423                            | 3.634                             | 23.142                | 8.99             | 0.779        |
| 36     | 129.434             | 1.423                            | 3.976                             | 25.173                | 10.722           | 0.779        |
| 37     | 120.954             | 1.423                            | 3.635                             | 23.006                | 8.934            | 0.777        |
| 38     | 129.434             | 1.423                            | 4                                 | 25.147                | 10.769           | 0.777        |
| 39     | 129.434             | 1.588                            | 3.634                             | 25.566                | 11.198           | 0.775        |
| 40     | 129.434             | 1.423                            | 4.071                             | 25.078                | 10.912           | 0.773        |
| 41     | 129.433             | 1.423                            | 4.078                             | 25.071                | 10.928           | 0.772        |
| 42     | 115.549             | 1.423                            | 3.634                             | 21.626                | 8.375            | 0.761        |
| 43     | 115.101             | 1.423                            | 3.634                             | 21.523                | 8.337            | 0.76         |
| 44     | 129.434             | 1.423                            | 4.305                             | 24.937                | 11.445           | 0.758        |
| 45     | 114.18              | 1.423                            | 3.634                             | 21.317                | 8.261            | 0.757        |
| 46     | 113.085             | 1.423                            | 3.634                             | 21.082                | 8.178            | 0.754        |
| 47     | 108.74              | 1.423                            | 3.634                             | 20.254                | 7.915            | 0.742        |
| 48     | 107.781             | 1.423                            | 3.634                             | 20.094                | 7.871            | 0.739        |
| 49     | 115.052             | 1.617                            | 3.634                             | 21.413                | 9.413            | 0.737        |
| 50     | 106.023             | 1.423                            | 3.634                             | 19.822                | 7.806            | 0.735        |
| 51     | 105.715             | 1.423                            | 3.634                             | 19.777                | 7.797            | 0.734        |
| 52     | 129.425             | 1.845                            | 3.634                             | 25.513                | 12.929           | 0.733        |
| 53     | 103.259             | 1.423                            | 3.634                             | 19.45                 | 7.74             | 0.728        |
| 54     | 102.421             | 1.423                            | 3.634                             | 19.35                 | 7.728            | 0.726        |
| 55     | 102.019             | 1.423                            | 3.634                             | 19.305                | 7.724            | 0.725        |
| 56     | 100.731             | 1.425                            | 3.634                             | 19.168                | 7.729            | 0.722        |
| 57     | 100.567             | 1.423                            | 4.039                             | 18.702                | 8.201            | 0.704        |
| 58     | 100.566             | 1.423                            | 4.4                               | 18.638                | 8.849            | 0.691        |

Data availability

Data will be made available on request.

References

Abdou, N., et al., 2021. Multi-objective optimization of passive energy efficiency measures for net-zero energy building in Morocco. *Build. Environ.* 204, 108141.

Adib, M., Nasiri, F., Haghighat, F., 2023. Integrating wind energy and compressed air energy storage for remote communities: a bi-level programming approach. *J. Energy Storage* 72, 108496.

Alirahmi, S.M., Assareh, E., 2020. Energy, exergy, and exergoeconomics (3E) analysis and multi-objective optimization of a multi-generation energy system for day and

night time power generation-Case study: Dezful city. *Int. J. Hydrogen Energy* 45 (56), 31555–31573.

Alirahmi, S.M., et al., 2021. A comprehensive techno-economic analysis and multi-criteria optimization of a compressed air energy storage (CAES) hybridized with solar and desalination units. *Energy Convers. Manag.* 236, 114053.

Aljashaami, B.A., et al., 2024. Recent improvements to heating, ventilation, and cooling technologies for buildings based on renewable energy to achieve zero-energy buildings: a systematic review. *Results Eng.*, 102769

Allaix, D.L., Carbone, V.I., 2011. An improvement of the response surface method. *Struct. Saf.* 33 (2), 165–172.

Almatrafi, E., Khaliq, A., 2021. Investigation of a novel solar powered trigeneration system for simultaneous production of electricity, heating, and refrigeration below freezing. *J. Sol. Energy Eng.* 143 (6), 061009.

Arshad, K., et al., 2024. Air pollution and climate change as grand challenges to sustainability. *Sci. Total Environ.*, 172370

- Assareh, E., et al., 2024a. A proposal on a co-generation system accompanied with phase change material to supply energy demand of a hospital to make it a zero energy building (ZEB). *Energy Build.* 318, 114478.
- Assareh, E., et al., 2024b. A newly application of Organic Rankine Cycle for building energy management with cooling heating power hydrogen liquefaction generation-South Korea. *Energy Nexus* 13, 100281.
- Assareh, E., et al., 2025a. Application of a multi-objective approach integrating solar-wind co-generation with response surface method to optimize zero-energy buildings. *Appl. Therm. Eng.*, 125637.
- Assareh, E., et al., 2025b. Optimizing solar photovoltaic farm-based cogeneration systems with artificial intelligence (AI) and Cascade compressed air energy storage for stable power generation and peak shaving: a Japan-focused case study. *Appl. Energy* 377, 124468.
- Azuza, A., et al., 2024. Review of cost objective functions in multi-objective optimisation analysis of buildings. *Renew. Sustain. Energy Rev.* 191, 114101.
- Baniasadi, E., et al., 2023. Exergy-economic analysis of a solar-geothermal combined cooling, heating, power and water generation system for a zero-energy building. *Int. J. Hydrogen Energy* 48 (99), 39064–39083.
- Barber, K.A., Krarti, M., 2022. A review of optimization based tools for design and control of building energy systems. *Renew. Sustain. Energy Rev.* 160, 112359.
- Bellos, E., Tzivanidis, C., 2019. Evaluation of a solar driven trigeneration system with conventional and new criteria. *Int. J. Sustain. Energy* 38 (3), 238–252.
- Buonomano, A., et al., 2023. Solar-assisted district heating networks: development and experimental validation of a novel simulation tool for the energy optimization. *Energy Convers. Manag.* 288, 117133.
- Cao, Y., et al., 2020. A novel multi-objective spiral optimization algorithm for an innovative solar/biomass-based multi-generation energy system: 3E analyses, and optimization algorithms comparison. *Energy Convers. Manag.* 219, 112961.
- Chandel, R., et al., 2022. Prospects of sustainable photovoltaic powered thermoelectric cooling in zero energy buildings: a review. *Int. J. Energy Res.* 46 (14), 19319–19340.
- Chen, B.-S., 2023. Multi-Objective Optimization System Designs and Their Applications. CRC Press.
- Christensen, C., et al., 2005. BEopt: Software for Identifying Optimal Building Designs on the Path to Zero Net Energy. National Renewable Energy Lab., Golden, CO (US).
- Christensen, C., et al., 2006. BEopt (TM) Software for Building Energy Optimization: Features and Capabilities. National Renewable Energy Lab.(NREL), Golden, CO (United States).
- Colakoglu, M., Durmayaz, A., 2022a. Energy, exergy, economic and emission saving analysis and multiobjective optimization of a new multi-generation system based on a solar tower with triple combined power cycle. *Sustain. Energy Technol. Assessments* 52, 102289.
- Colakoglu, M., Durmayaz, A., 2022b. Multiobjective optimization of a novel solar tower-based gas turbine-driven multi-generation plant with energy, exergy, economic, and environmental impact analysis. *J. Energy Resour. Technol.* 144 (5), 051302.
- Dashtizadeh, E., Houshfar, E., 2025. Multi-objective optimization and 4E analysis of a multi-generation system for hydrogen production using WHR in cement plants. *Results Eng.* 25, 103845.
- Delpisheh, M., et al., 2021. Desalinated water and hydrogen generation from seawater via a desalination unit and a low temperature electrolysis using a novel solar-based setup. *Int. J. Hydrogen Energy* 46 (10), 7211–7229.
- Din, I., Rosen, M.A., Ahmadi, P., 2017. Optimization of Energy Systems. John Wiley & Sons.
- Esmailion, F., et al., 2022. Design, analysis, and optimization of a novel poly-generation system powered by solar and wind energy. *Desalination* 543, 116119.
- ESMAP, Energy Sector Management Assistance Program, 2024. Energy Sector Management Assistance Program (ESMAP).
- Gjoka, K., Rismanchi, B., Crawford, R.H., 2024. Fifth-generation district heating and cooling: opportunities and implementation challenges in a mild climate. *Energy* 286, 129525.
- Gonçalves, A.C., et al., 2024. Extreme weather events on energy systems: a comprehensive review on impacts, mitigation, and adaptation measures. *Sust. Energy Res.* 11 (1), 4.
- GoogleEarth, 2025. Azad University of Dezful. GoogleEarth, Iran.
- IEA, 2024. The breakthrough agenda report. In: *THE BREAKTHROUGH AGENDA REPORT 2024*. INTERNATIONAL ENERGY AGENCY (IEA).
- Jaysawal, R.K., et al., 2022. Concept of net zero energy buildings (NZEB)-A literature review. *Clean. Eng. Technol.* 11, 100582.
- Korpeh, M., et al., 2024. 4E analysis and optimization of a novel hybrid biomass-solar system: focusing on peak load management and environmental emissions. *Process Saf. Environ. Prot.* 181, 452–468.
- Kroeger, T., et al., 2014. Reforestation as a novel abatement and compliance measure for ground-level ozone. *Proc. Natl. Acad. Sci.* 111 (40), E4204–E4213.
- Kyriaki, E., Giama, E., 2022. Hybrid solar photovoltaic thermal systems in Nearly-Zero Energy Buildings: the case of a residential building in Greece. *Int. J. Sustain. Energy* 41 (10), 1521–1532.
- Lamnatou, C., Chemisana, D., Cristofari, C., 2022. Smart grids and smart technologies in relation to photovoltaics, storage systems, buildings and the environment. *Renew. Energy* 185, 1376–1391.
- Li, D.H., Yang, L., Lam, J.C., 2013. Zero energy buildings and sustainable development implications—A review. *Energy* 54, 1–10.
- Li, D.-Q., et al., 2016. Response surface methods for slope reliability analysis: review and comparison. *Eng. Geol.* 203, 3–14.
- Li, F., et al., 2023. Study on characteristics of photovoltaic and photothermal coupling compressed air energy storage system. *Process Saf. Environ. Prot.* 178, 147–155.
- Lou, H.-L., Hsieh, S.-H., 2024. Towards zero: a review on strategies in achieving net-zero-energy and net-zero-carbon buildings. *Sustainability* 16 (11), 4735.
- Lykas, P., et al., 2023. A comprehensive review of solar-driven multigeneration systems with hydrogen production. *Int. J. Hydrogen Energy* 48 (2), 437–477.
- Maleki Dastjerdi, S., Ardehali, A., Naseryar, F., 2024. Comprehensive design and transient analysis of novel off-grid zero energy and nearly zero emission building with hydrogen-integrated storage system. *Energy Technol.* 12 (3), 2300827.
- Mehrpooya, M., et al., 2021. Investigation of a hybrid solar thermochemical water-splitting hydrogen production cycle and coal-fueled molten carbonate fuel cell power plant. *Sustain. Energy Technol. Assessments* 47, 101458.
- Melo, F.M., Pina, E.A., Carvalho, M., 2021. Optimization and sensitivity analyses of a combined cooling, heat and power system for a residential building. *Therm. Sci.* 25 (5 Part B), 3969–3986.
- Meteotest. Meteororm: Global meteorological data for any location [cited 2024 7 October]; Available from: <https://meteororm.com/en/>.
- Mobayen, S., et al., 2025. Multi-functional hybrid energy system for zero-energy residential buildings: integrating hydrogen production and renewable energy solutions. *Int. J. Hydrogen Energy* 102, 647–672.
- Mohammadi, K., et al., 2020. A comprehensive review of solar only and hybrid solar driven multigeneration systems: Classifications, benefits, design and prospective. *Appl. Energy* 268, 114940.
- Mohammadikhah, F., Javaherdeh, K., Mahmoudimehr, J., 2021. Thermodynamic analysis and multi-objective optimization of a new biomass-driven multi-generation system for zero energy buildings. *Energy Syst.* 12 (1), 157–180.
- Mohtasim, M.S., et al., 2025. Hybrid renewable multi-generation system optimization: Attaining sustainable development goals. *Renew. Sustain. Energy Rev.* 212, 115415.
- Mouaky, A., Rachek, A., 2024. Multi-objective optimization of a solar-biomass multi-generation system with dual-stage desalination for brine minimization. *J. Clean. Prod.* 477, 143849.
- Mungbua, C., et al., 2024. Enhancing cost-efficiency in achieving near-zero energy performance through integrated photovoltaic retrofit solutions. *Appl. Energy* 367, 123307.
- Nam, A.K., et al., 2025. Designing and multi-objective optimization of a novel multigenerational system based on a geothermal energy resource from the perspective of 4E analysis. *Appl. Therm. Eng.* 258, 124673.
- Nedaei, N., Azizi, S., Farshi, L.G., 2022. Performance assessment and multi-objective optimization of a multi-generation system based on solar tower power: a case study in Dubai, UAE. *Process Saf. Environ. Prot.* 161, 295–315.
- Nikitin, A., et al., 2023. Energy, exergy, economic and environmental (4E) analysis using a renewable multi-generation system in a near-zero energy building with hot water and hydrogen storage systems. *J. Energy Storage* 62, 106794.
- Noro, M., Mancin, S., Riehl, R., 2021. Energy and economic sustainability of a trigeneration solar system using radiative cooling in mediterranean climate. *Sustainability* 13 (20), 11446.
- Pereira, J.L.J., et al., 2022. A review of multi-objective optimization: methods and algorithms in mechanical engineering problems. *Arch. Comput. Methods Eng.* 29 (4), 2285–2308.
- Rhodes, J.D., et al., 2015. Using BEopt (EnergyPlus) with energy audits and surveys to predict actual residential energy usage. *Energy Build.* 86, 808–816.
- Saadmohammadi, B., Sajadi, B., 2024. 4E analysis and tri-objective optimization of a novel solar 4th cogeneration system for a smart residential building in various climates of Iran. *Energy Convers. Manag.* 303, 118177.
- Sadat, S.Z.H., et al., 2024. Aligning Net zero energy, carbon Neutrality, and regenerative concepts: an exemplary study of sustainable architectural practices. *J. Build. Eng.* 90, 109414.
- Sami, S., Gholizadeh, M., Deymi-Dashtebayaz, M., 2024. An applicable multi-generation system for different climates from energy, exergy, exergoeconomic, economic, and environmental (5E) perspectives. *Sustain. Cities Soc.* 100, 105057.
- Sarvar-Ardeh, S., et al., 2024. Recent advances in the applications of solar-driven co-generation systems for heat, freshwater and power. *Renew. Energy*, 120256.
- Shayan, M.E., 2020. Solar energy and its purpose in net-zero energy building. *Zero-Energy Buildings—New Approaches and Technologies* 14.
- Sretenovic, A., 2013. Analysis of Energy Use at University Campus. Institutt for energi-og prosesseteknikk.
- Stat-Ease, 2021. Design-Expert Version 13. Stat-Ease, Inc., Minneapolis, MN, USA.
- Sullivan, W.G., Wicks, E.M., Koelling, C.P., 2015. Engineering Economy. Pearson.
- Susaimanickam, A., Manickam, P., Joseph, A.A., 2023. A comprehensive review on RSM-coupled optimization techniques and its applications. *Arch. Comput. Methods Eng.* 30 (8), 4831–4853.
- Tajalli-Ardekani, E., et al., 2024. A Rome district transition towards optimal and sustainable heat and power generation. *Appl. Therm. Eng.* 255, 124001.
- Temiz, M., Dincer, I., 2022. Design and analysis of a floating photovoltaic based energy system with underground energy storage options for remote communities. *J. Energy Storage* 55, 105733.
- Tool, B.B.B.E.O., 2024. 5 best energy modeling software tools for net-zero buildings: Digital architects of sustainability. *Energy*.
- UNEP, 2023. 2023 Global Status Report for Buildings and Construction. United Nations Environment Programme (UNEP).
- Wang, P., et al., 2024a. A multi-generation system with integrated solar energy, combining energy storage, cooling, heat, and hydrogen production functionalities: mathematical model and thermo-economic analysis. *Renew. Energy*, 120812.
- Wang, S., et al., 2024b. An improved parameter identification and radial basis correction-differential support vector machine strategies for state-of-charge estimation of urban-transportation-electric-vehicle lithium-ion batteries. *J. Energy Storage* 80, 110222.
- Wang, S., et al., 2024c. An accurate state-of-charge estimation of lithium-ion batteries based on improved particle swarm optimization-adaptive square root cubature kalman filter. *J. Power Sources* 624, 235594.

- Wang, S., et al., 2024d. An innovative square root-untraced Kalman filtering strategy with full-parameter online identification for state of power evaluation of lithium-ion batteries. *J. Energy Storage* 104, 114555.
- Xu, Y., Leonforte, F., Del Pero, C., 2024. District multi-energy systems: a comprehensive review of configurations, technologies, and performances. *Build. Environ.*, 111318
- Yadav, V.K., Sarkar, J., Ghosh, P., 2023. Thermodynamic, economic and environmental analyses of novel concentrated solar-PV-thermal integrated combined power, cooling and desalination system. *Desalination* 563, 116721.
- Ye, A., et al., 2023. Using solar energy to achieve near-zero energy buildings in Tibetan Plateau. *Renew. Energy* 218, 119347.
- Zhang, J., et al., 2024a. Multi-objective optimization design of a solar-powered integrated multi-generation system based on combined SCO<sub>2</sub> Brayton cycle and ORC using machine learning approach. *Appl. Therm. Eng.*, 123684
- Zhang, Y., et al., 2024b. Thermodynamic and economic analysis of a novel thermoelectric-hydrogen co-generation system combining compressed air energy storage and chemical energy. *Energy* 286, 129508.
- Zhao, X., et al., 2024. Optimization and exergoeconomic analysis of a solar-powered ORC-VCR-CCHP system based on a ternary refrigerant selection model. *Energy* 290, 129976.